ADDIS ABABA UNIVERSITY

ADDIS ABABA INSTITUTE OF TECHNOLOGY

AFRICAN RAILWAY CENTER OF EXCELLENCE

EFFECT OF TRAIN LOADING FLUCTUATION ON THE DAMAGE OF RAIL CATENARY CONTACT CONDUCTOR WIRE

A thesis in Railway Engineering (Rolling Stock)

By

Egide Niringiyimana

March 08, 2021

A

Thesis

Submitted to the School of Graduate Studies of Addis University in Partial Fulfilment for the Degree of Master of Science in Railway Engineering, Rolling Stock.

A

Dissertation

Presented to the African Railway Center of

Excellence Graduate College at Addis Ababa University

In Partial Fulfillment of Requirements

For the Degree of Masters of Science.

Addis Ababa Institute of Technology

Major: Railway Engineering, Rolling Stock Design

Under the Supervision of Dr. Celestin Nkundineza

Addis Ababa, Ethiopia

Email: niringiyimanegide@gmail.com

March 08, 2021

The undersigned members of Addis Ababa Institut of Technology under the department of Railway Engineering have examined the thesis entitled '**EFFECT OF TRAIN LOADING FLUCTUATION ON THE DAMAGE OF RAIL CATENARY CONTACT CONDUCTOR WIRE'** presented by **Egide Niringiyimana**, a candidate for the degree of **Mater of Science** in **Rolling Stocks Design** and hereby certify that it is worth of acceptance.

Board of Examiners

Dr. Celestin Nkundineza	……	……..
Advisor	Signature	Date
Dr. Kamil Dino Adem	……..	…..……
External Examiner	Signature	Date
Dr. Daniel Tilahun Redda	……	…….
Internal Examiner	Signature	Date
Dr. Abraham Gebre	……..**.....**	……**.....**
Chair Person of Department	Signature	Date

Graduate Committee (DGC)

Undertaking

I certify that the research work entitled "Effect of Train Loading Fluctuation on the Damage of Rail Catenary Contact Conductor Wire " is my own work .The work has not been presented elsewhere for assessment .Where material has been used from other sources it has been properly acknowledged/referenced.

……

Student Signature

Egide Niringiyimana

Abstract

With current rise of climate change worldwide, transport industry contributes up to 21% of the world's total Green House Gases (GHG). In addition to that developing cities are facing great changes in urbanization, population growth and environmental concerns. In this case, railway transportation is a top contender on land transport mode to achieve sustainable mobility in fast growing cities. For railway operation, apart from wheel-rail contact, the catenary pantograph has a very high initial investment cost as well as associated maintenance cost. It is important to monitor the damage evolution of the catenary components for developing better maintenance strategies. Embedding on the development of computer technologies, the current research applies numerical analysis, 3D modelling and simulation approaches using commercialized software packages (e.g. Abaqus, Matlab, solid works and python) and co-Simulation technics to investigate the effect of train loading fluctuations on the damage of rail catenary contact conductor wire. With reference to Addis Ababa Light Rail Transit Service (AA-LRTS), the power and current drawn by the running train were calculated. Then the heat losses in the conductor wire were obtained with respect to train location on the line. This procedure was followed by thermal analysis that allowed us to obtain temperature rise in the conductor. The temperature results were used as the inputs in the dynamic explicit finite element model of the coupled catenary and sliding pantograph. From the finite element analysis, different quantities such as contact forces and pressures, temperature rise because of friction between sliding parts, and deflections of conductor wire were obtained. Increase in loads from empty to overload car resulted in increase of current drawn by 47% which increases the temperature of the mating parts from 20^0C to 100^0C that in-turn results in average increase by 0.24% and 0.31% of the contact pressures and contact forces respectively. The latter were the input parameters in Archard wear model for calculating wear depth and the volume of material removed from the catenary contact conductor wire. It was observed that at different scenarios of train passenger capacity of empty, half, full and overload capacities, a train experiences an increase in energy consumption, which results in an average increase of 0.20% of the contact wire wear depth and 0.29% of the total volume of the material removed.

***Key words*:** Light Rail Transit, co-simulation, pantograph, catenary system, contact pressures, Archard wear model.

Acknowledgment

I take this opportunity to thank every person who made me accomplishing my MSc studies at Addis Ababa University/Addis Ababa Institute of Technology/African Railway Center of Excellence from 2018 till now. First and foremost I would like to thank my Supervisor Dr. Celestin Nkundineza. He guided me into the academic research area of effect of train loading fluctuation on the damage of rail catenary contact conductor wire from the perspective of Finite Element Methods. He taught me how to be a good researcher. His weekly meeting and fruitful discussion made me working hard and get familiar with research work. His words and prompt responses and feedback to any questions and challenges I faced during the research trained me to be patient, responsible and stay focused.

I also thank Addis Ababa University both teaching and non-teaching staff for their tremendous advice and support during my studying period at the University. The conducive academic environment they availed made me feeling motivated and being successful.

The author would like to also acknowledge the data provided by Addis Ababa Light Rail Transit Services, they are helpful in the performance of the undertaken research.

My warmth thanks are extended to my colleagues and friends in the department of Railway Engineering. The productive discussions, studying encouragements and joyful conversations and entertainment we had together made my life vibrant at the campus.

I extremely express my special gratitude to the DAAD (Germany Academic Exchange services) to offer the scholarship opportunity. This funded my studies at the Addis Ababa University and made me conducting my research in both mentally and physically humor.

Finally, my heartfelt thanks goes to my entire family member; my parents, my brother and sister, and my relatives who cared about me all the time . They tirelessly supported me, encouraged me and advanced my progress in my years of studies.

Table of Content

List of Tables

List of Figures

List of Acronyms

DAAD: Deutscher Akademischer Austauschdienst

GHG: Green House Gas

BMT: Bus Mass Transit

LRT: Light Rail Transit

EMU: Electrical Multiple Unit

OCS: Overhead Contact System

AA-LRTS: Addis Ababa Light Rail Transit Services

FEM: Finite Element Method

FE: Finite Element

OLE: Overhead Line Electrification

BC: Black Carbon

CBs: Carbon Blacks

MCT: Motor Controlled Thyristor

FEA: Finite Element Analysis

DoF: Degree of Freedom

1 Introduction

Nowadays, with a dramatic increase in climate change worldwide and transport industry contributing to 21% of the World's total Green House Gases (GHG) [1], developing cities are currently facing a great change in urbanization, population growth and environmental concerns that highly push in deed of sustainable mobility. In this case railroad transportation is a top contender for land transport modes because of its advantages such as environmental friendliness, high energy efficiency, safety, ride comfort and stability, increased speeds, etc. For promoting emission free transportation systems and meet the ever increasing traveling demands in growing cities. There is a need of public transport that use clean energy over private vehicles. Mass transit systems, such as Bus Mass Transit (BMT), metros, trams and Light Rail Transit (LRT), provide large passenger capacity (i.e. High passenger per direction per hour), unique exclusive right of way, reduced traveling times, reduced congestion, etc. Among other mass transit systems, Light Rail Transit has gained a considerable amount of attention over the past few decades. LRT may use diesel-electric power source (i.e. Diesel-Electric trains) or pure electrical power source (i.e. Electrical Multiple Unit: EMU). Diesel- electric trains are heavy and still use diesel internal combustion engine which not only requires high maintenance cost but also contributes to environmental pollution. As of today, to power electric trains, technologies such as third rails/contact shoe, Magnetic Levitation (commonly abridged as Maglev) and overhead contact systems (OCS) are used. OCS should be an elaborate design which can ensure good quality of electricity transmission at relatively high speeds to power LRT electrical trains. It is worth to note that OCS are safe (meaning to say pedestrians are not exposed to live electrical high voltage as compared to third rail), simple to install, and easy to maintain. OCS is fixed over the railway tracks with the contact wire above for the collection of electricity by the pantographs which are mounted on the roof of trains. The pantograph draws electrical current while sliding along the contact wire of the catenary basing on a pantograph-catenary system interaction phenomenon.

The electrical current is returned through the train wheels back to the rails. As the rails and wheels are always in good contact during operation, the contact between pantograph and catenary becomes one of the key issues for the reliability of railway operation. Therefore, it is always necessary to perform careful investigation once there are some technical changes to the pantograph-catenary systems to ensure safety, reliability and feasibility.

The abundant undertaken researches on the dynamic interaction of the pantograph catenary systems showed that on-track tests are not only costly and time-consuming but sometimes even risky. In addition, because the pantograph-catenary system is a complex structure and is subjected to a great number of influencing factors, not all details of the system are observable or detectable. With the development of computer technology, it has become more and more popular to study the pantograph-catenary system through numerical methods.

Numerical studies allow manageable and observable conditions to perform very detailed investigation, which is sometimes very hard or even impossible to do in a real test. Although numerical studies of the pantograph-catenary system are effective and efficient, it always requires proper identification of the system parameters and the model should be very close to the real pantograph-catenary system. The present research investigates the effects that the passenger capacity fluctuation has on the train power consumption and relate it to the behavior of the pantograph-catenary interaction in order to estimate the wear of the contact wire that is caused by electromechanical effects. To make the research feasible, AA-LRTS is referenced to gather some factual information regarding modelling parameters, contact wire condition and its maintenance strategies, train performance and reliability, and train passenger flow, especially in pick periods.

AAL-RTS is a public transportation company which operates train lines in Addis Ababa, The capital city of the Federal Democratic Republic of Ethiopia since the year of 2015. AA-LRTS offers its service with 41 trains which operate on a 2 train's lines; North-South and East-West train lines. North-south line extends to a distance of 16.9 km while East-West line has a coverage of 17.4 km. Both train lines share a common track section of 2.7km covering stations between St. Lideta and Stadium train stations. With both lines combined, AA-LRTS is capable of transporting 60,000 passengers a day. It was forecasted that the track section laying between St. Lideta and Leghar stations experiences a high level of passengers flow during the train operation [2]. It is believed that the high passenger flow may promote the overloading of the train beyond its designed capacity. Various research conducted proved that loading a train beyond its capacity not only lead to the excessive power consumption and headway inconsistency, it also contributes to the environment pollution [3],[4][5]. The previous researches did not consider the impact the train overcapacity has on the degradation of power supply components i.e. contact wire and pantograph strip). Therefore, the current research is conducted to fill this void.

The research analyses the wear mechanism of the contact wire used at AA-LRTS. Matlab is used to numerically solve the train power flow equations. Finite Element Method (FEM) is utilized to study the dynamic behavior of the catenary-pantograph interaction. Archard wear model is applied to perform wear analysis of the contact wire as a results of friction between the mating components in motion (contact wire and pantograph contact strip), temperature variation of the contact wire and contact strip during current collection as a result of train over capacity.

1.1 Background

This section described the background of the pantograph- catenary system. Since the past few years, the evolution of railway industry has considered the pantograph-catenary system technology as the effective and efficient method to supply the electrical trains with the electrical current. As the name reveals it, the pantograph-catenary system consist two emerging sub-system; pantograph and catenary.

Problems of pantograph-catenary systems

During operation of train with Overhead Contact Systems, different influencing factors such as contact force fluctuation, high sliding speed, high electrical load and environmental factors may emerge. The aforementioned factors possibly contribute to the wear of pantograph carbon strip and contact wire of the catenary, arcing between pantograph and catenary and even structure damage of the pantograph and catenary system once no attention is drawn. As a solution, the contact force must be optimized, otherwise there would be some problems that arise. Too high contact force would lead to excessive mechanical wear and thus shorten the service life of the entire system. Too low contact force is also a concern which can cause poor quality of current collection and electrical discharge, which contributes to electrical erosion [1].It is important to note that other train characteristics such as empty car, train overloading, train working speed, number of axles on a train and the drag coefficient affect the train power and energy consumption [3]. Train carrying capacity fluctuation especially in pick hours is thought to have a great impact on train power consumption. This results in contact wire temperature fluctuation which results in its degradation. Different degradations phenomena raise in pantograph- catenary systems including contact strip and contact wire wear and tear, railway line damage, contact wire and contact strip material erosion. See Figure 1.

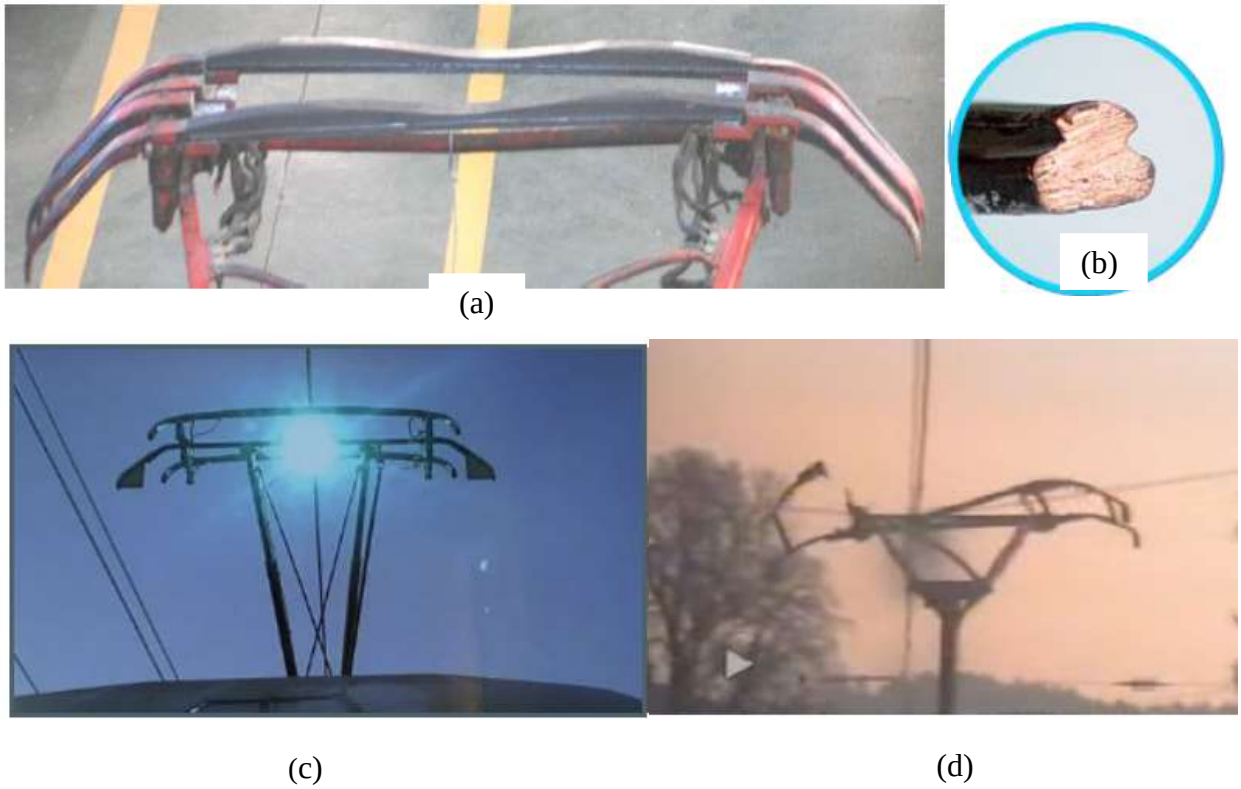

Figure 1. Technical concerns of pantograph-catenary system [6].(a) Wear on pantograph ; (b) Wear on contact wire; (c) Arcing between pantograph and catenary; (d) Structure damage of the pantograph-catenary system.

Current technology in Light Rail transit and pantograph and catenary system configuration at AA-LRT

Addis Ababa Light Rail Transit is an electrified railway using OCS to feed electrical current to electrical motors to move the train. Compound contact wire type and Z-shaped pantograph are two involved components to supply and collect current in nowadays electrified railway [7],[8],[9].

- **AA-LRT Pantograph design**

AA-LRT uses Electrical Multiple Unit (EMU) trains. AA-LRT EMU trains consist of power car carrying a Z-shaped pantograph which is the most common type of pantograph used in today's railways and draws electrical current from overhead line electrification, Motor car, which carry traction motors and driving car containing the driver cab to control the train. Figure 2 represents the type of pantograph used at AA-LRT.

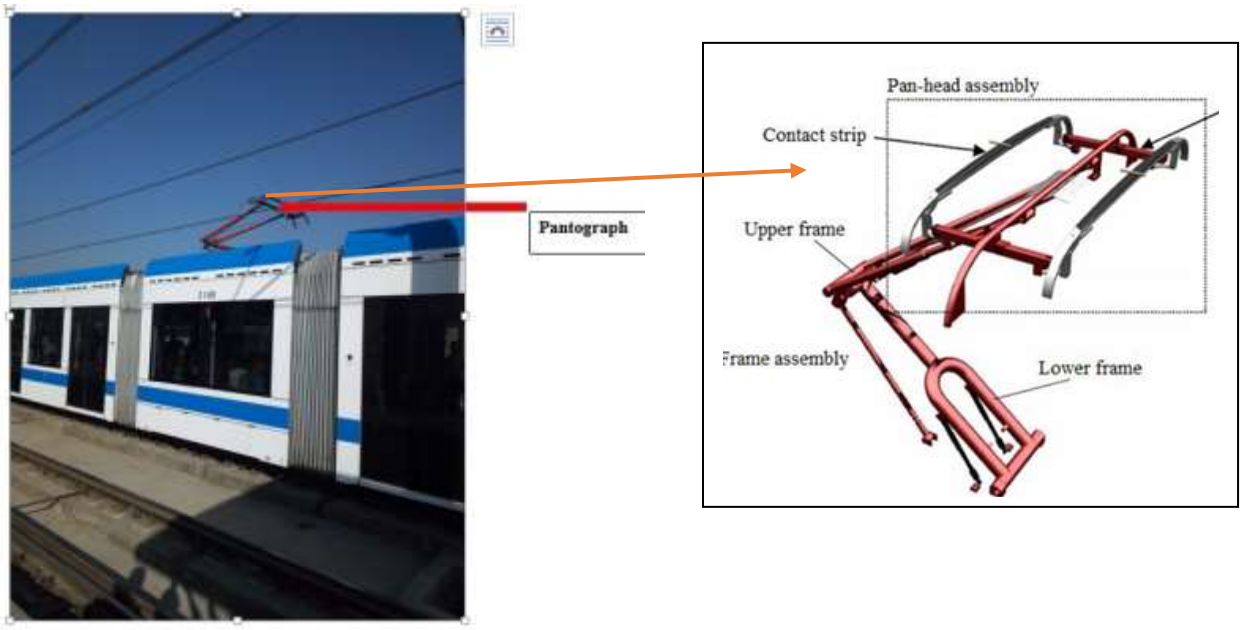

Figure 2. AA-LRTS EMU train With Z shaped Pantograph

- **AA-LRTS Overhead Catenary system design**

Different types of overhead catenary systems exist, depending on the speed of the train and the voltage level. An overhead catenary system is composed of one or several wire conductors hung over the track. One of them is the contact wire, it is in contact with the train's current collector, called the pantograph mounted on the roof of the train. In order to guaranty a good contact, the contact wire should have an even elasticity distribution and therefore has to be hold by a messenger wire and droppers. Different types of catenary technologies are in use nowadays [9]. A system comprising only a single catenary cable and a contact wire supported by droppers is described as a simple catenary system, this has the disadvantage of when loaded vertically by the up-lift force of a passing pantograph, and the vertical displacement near the center of a span is greater than that near the support. To appreciably reduce the said effect, a stitched catenary is designed. The most advanced yet complicated, and consequently more expensive, catenary system is known as 'compound' catenary. It employs a continuous auxiliary catenary supported from the main catenary and in turn supporting the contact wire [10].

Addis Ababa Light Rail Transit uses compound catenary technology. The catenary is a well-suspended overhead power line above the track .Basically, the catenary consists of contact wire,

catenary wire (messenger wire), droppers connecting the contact wire to the catenary wire and supporting, and suspension structures at the poles. Figure 3 shows the component of catenary system used at AA-LRTS (i.e. catenary system at AA-LRTS, Autobus Tera Station).

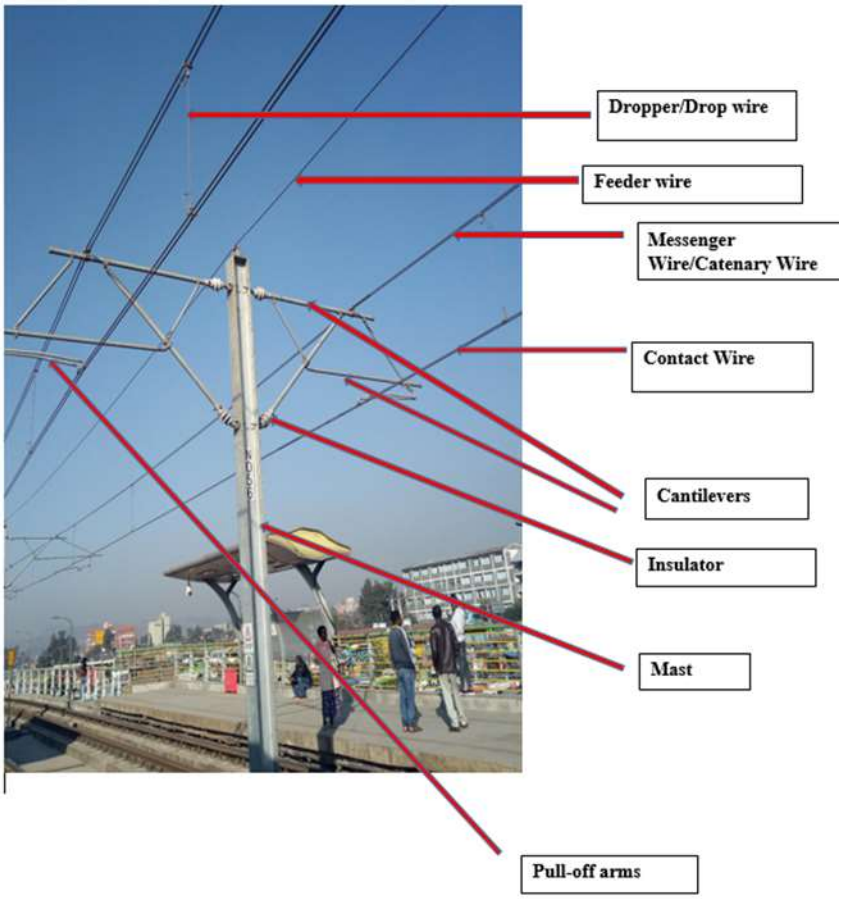

Figure 3. Components of catenary system at AA-LRTS, Autobus Tera Railway station

Overview of adapted approaches for investigating wear behavior in OCS

Back in the days, experimental approaches were helpful to investigate the dynamic behaviors of pantograph-catenary interactions. A real pantograph and catenary systems were to be established in sort of laboratory to study the real time wear phenomena of the railway system components taking into account numerous affecting factors such as train routes, vehicles operating parameters, number of vehicle passing in case of contact wire life span degradation modeling. The experiments test rig using pin-on disc technology were the popular approach. The pin sample was made of carbon strip, which is a kind of typical commercial pantograph strip materials used in electrified railways. The disc sample was made of a pure copper, which is a type of contact wire materials used in electrified railways [12],[12].

A pin-on disc tribometer was used to study the pantograph-catenary wear behavior [11]. However, physical models of real pantograph, catenary, pin-on-disc testing apparatus are dominated by 3D modeling in computer with the dedicated software packages. It is no doubt to highlight that experiments approaches are not only expensive but also are complicated and time consuming. The complexity of on field experiments and measurements are surpassed by the simulations. The latter provide more details and more facilities to play around different parameters involved while carrying out an investigation on railway components operating behavior which seemed impossible when conducting experiments.

1.2 Statement of the problem

The variation of passenger railway vehicle loads is an inevitable phenomenon in the railway industry. It is a well-known fact that fluctuations in vehicle loads influences the power consumption of the tractive system. At high loading capacities it is expected that the tractive system consumes high power and vice versa. Previous researchers investigated the influence of trains route and operating parameters on the power consumption of railway vehicle [5]. Others investigated the wear mechanisms of OCS materials using experiments with sample materials by studying the tribological behavior of the carbon/copper sliding pair taking into account the current application [13]. Others used analytical methods to calculate dynamic behavior of OCS [14]. Others studied how the mechanism of vehicle body vibrations can affect the dynamic interaction in the OCS [15]

Based on the previous researches conducted, the effect of train energy consumption on the wear condition of the contact conductor wire was not tackled. It was revealed that the train energy consumption is affected by deferent train operation parameters such as the condition of the track, the driving speed, the passenger's capacity etc. Among others, the passengers' capacity fluctuation was found to have impact on the power consumed by the train and this causes the change in thermal behavior of the interacting elements (i.e. Pantograph strip catenary contact wire).

Our hypothesis is that the rate and magnitude of power drawn by a railway vehicle affects the thermal behavior of both the catenary and the pantograph contact strip. This in-turn influences the dynamic and contact wear behavior of the pantograph catenary system.

Embedding on the advantages of computer interventions in performing many studies on the aforementioned issues, the current research apply numerical analysis, 3D modelling and simulations approaches using commercialized software packages (e.g. Abaqus, Matlab, solid works) to investigate the influence of rail vehicles loading fluctuations on the wear and degradation modes of the contact wire of the catenary during train operation. Moreover, Archard wear model is adopted to calculate the contact wire wear depth and also to estimate the volume of material removal.

1.3 Research questions

Main research question

To what extent does the railway vehicle load fluctuation affects the wear and degradation of catenary system components.

Specific questions

- How does the change on the train loads influences the power consumption
- What is the variation of current drawn by the train at different loading capacities?
- What is the influence of increased current drawn by the train on the thermo-behaviour of both the pantograph and the contact wire?
- What is the influence of the power consumption rate on the sliding contact behavior of the catenary pantograph system?
- What is the influence of the railway vehicle loads on the wear volume and depth of the contact wire?

1.4 Objectives: main objective and specific objectives

Main objective

The focus of this study is an attempt to investigate the wear and degradation of the catenary wire taking into consideration some neglected factors/parameters such as the fluctuation of loading capacity.

Specific objectives

- To provide the solution of the power flow equation taking into consideration the variation in railway vehicle loads.
- To evaluate the railway vehicle loads with current drawn
- To calculated the temperature on the catenary pantograph interaction at different currents
- To calculate the wear depth and volume on the catenary contact wire at different loads

1.5 Scope/Delimitation

The current research investigates the effect of train passengers' capacity fluctuation on the wear behavior of the contact wire. The model parameters are blend of AA-LRTS parameters and the literature review data on the theme of the pantograph-catenary dynamic interaction phenomenon. The undertaken research only considers a constant speed and one train on the line. The FEM is limited to a line between two masts because of the limitation of computational resources, while analytical calculations are limited on a line between two feeding substations. It is suggested to use varying speeds and a combination of trains on the line for the future research for the sake of the current research enrichment.

1.6 Significance of the research

On any electrified railway, effective train operation depends on the power collection quality. Both the pantograph and the catenary play a major role in power collection quality of the electrical train. A careful investigation is imperial to ensure the operation worthy of moving train. In this regard, the conducted research provided a clear picture of how the fluctuation of passengers' loading capacity has an influence phenomenon of the wear behavior of the contact wire and this might be a relevant research to be based on so as to control the loading capacity of the train which in turn relief cycle cost of the railway infrastructure.

1.7 Research approach and organization of the thesis

It is revealed that experimental approaches do not provide enough rooms to easily study various operating scenarios of railway system components. With the booming of computer technologies, it is simple, cost effective and time manageable to investigate a lot of operating performances of railway system components at a time. Inefficient and tiring hand calculations to solve pantograph and catenary interaction equations of motion as well as railway electrical power flow equations were recently replaced

by numerical methods using computers algorithms. This research adopts numerical method to be able to account effects of different physical parameters on OCS.

Figure 4 highlights all the steps involved in this research and it consists of 5 chapters. After the introductory chapter, Chapter 2 is the Literature review. It gives an overview of recent researches on pantograph catenary interaction, pantograph carbons strip and contact wire wear mechanism, rail vehicles power consumption analysis, railway transportation environmental concerns and its impact to the ecology. The former also elucidates the research void on contact wire wear prediction as well its life span degradation taking into consideration of various rail vehicle operating parameters. Chapter 3 encompasses the methods used in this research. This chapter also shows the steps to undergo in order to cover the set objectives as portrayed in the elaborated conceptual frame work.

Figure 4. Throughout this chapter also, the numerical modeling of the train power flow is given, a 3D finite element (FE) model of the pantograph-catenary is depicted, the pantograph-catenary interaction simulation input parameters are listed and the required software packages for pantograph and catenary Finite Element and numerical Analysis are highlighted. Moreover, the Archard wear model useful for the calculation of contact wire wear depth as well as the volume of material removed is clarified in this section. In chapter 4, the obtained results from FE of the pantograph-catenary dynamics and the contact wire wear analysis are discussed. Furthermore, the method forward for the obtained results validation is demonstrated throughout this chapter. Finally, in Chapter 5, some conclusions are drawn based on the obtained results and the recommendation and the future researches are proposed

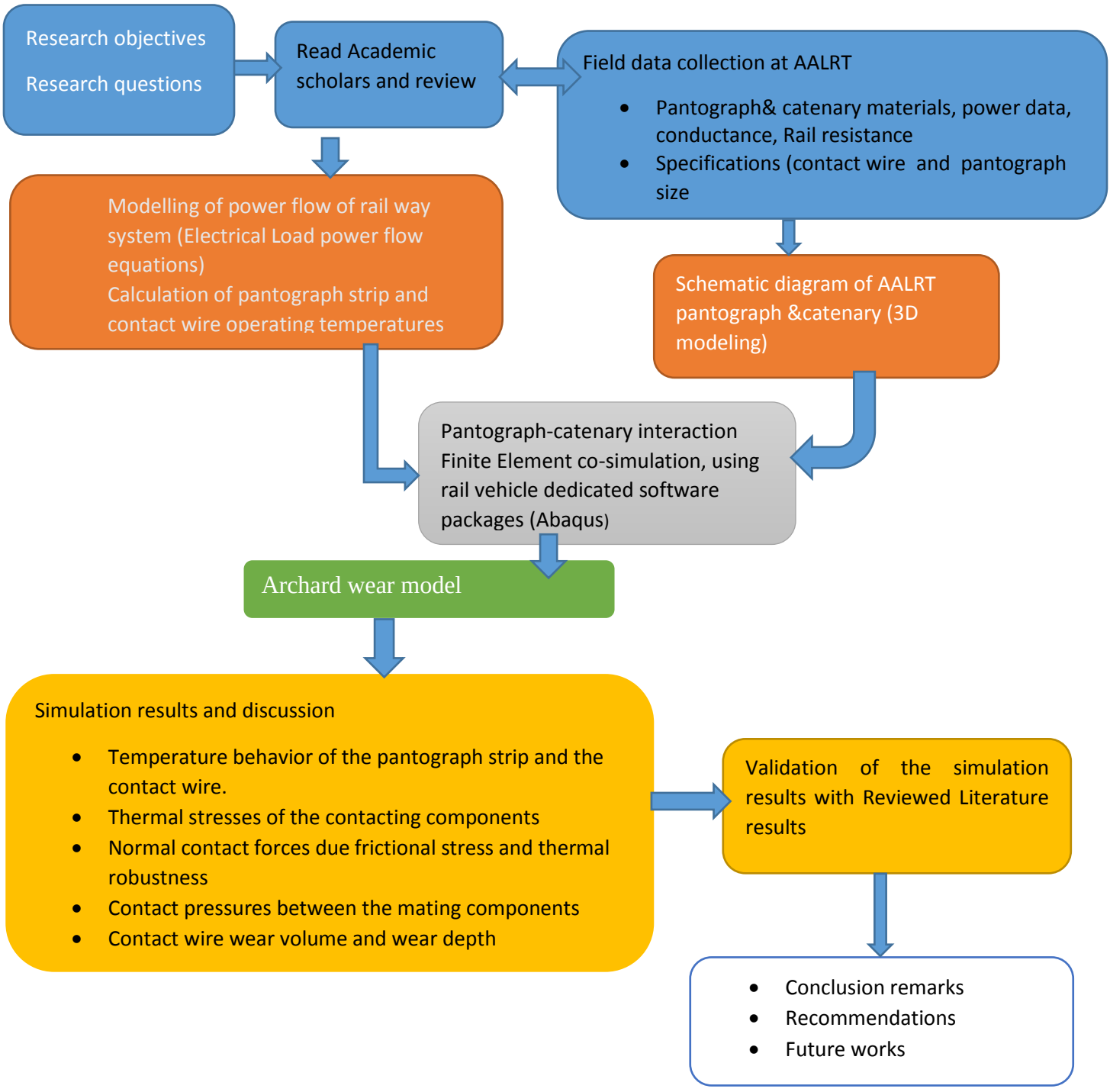

Figure 4. Conceptual frame work.

2 Literature Review

Currently, with the development of railway industry, the wear of the pantograph-conduct wire contact pair and the dynamics of the pantograph-catenary interaction is a big concern for both the system designers and manufacture operators[9]. Moreover, the dynamics of the pantograph-catenary has become one of the major factors, which limit the operating speed of the railway lines and determine the service life of the key components[16]. As of today, many numerical studies have been carried out and much progress has been made aiming for higher operational speed, lower maintenance cost, low energy consumption, ecology preserve, higher reliability, more flexibility and reduction of the wear of both pantograph carbon strip and conductor wire.

Nåvika et al. [17] studied the dynamic comparison of a railway catenary section upgrade by field measurement assessments. Haugland [18] worked on the dynamic behavior of a full scale laboratory model of a catenary system by measurements and numerical analysis. Juan de Dios et al. [19], analyzed the capability of non-specific simulation software for studying the dynamic interaction between pantograph and rigid of the overhead conduct rail .Grandin et al. [20], studied the influence of mechanical and electrical load on a copper/copper-graphite sliding electrical contact and wear phenomena and tribo film formation of copper/copper-graphite sliding electrical contact materials. Zhou [21], investigated the dynamic performance and parameter optimization design of pantograph and catenary system. Xin et al. [22] worked on the condition based railway pantograph dynamic behavior measurement and fault diagnosis. Xiong et al. [23] conducted an experiment on arc erosion wear characteristics and mechanisms of pure carbon strip against copper under arcing conditions. Bucca and Collina [24] studied the electromechanical interaction between carbon-based pantograph strip and copper contact wire using a heuristic wear model. The wear results showed high values of worn area in the section under suspension of about 20% to 30% with respect to the section at mid-span. It was also found that if the wire irregularities is considered, the lower wire irregularities produce 10% less wear while high level wire irregularities produce 30% to 40% more wear compared to low level of irregularities.

2.1 Material behavior and wear mechanisms of overhead contact systems (current findings)

Several contact wire materials were developed. Taking reference to EN 50149, there are different materials for contact wire such as Cu Mg0, 2, Cu Mg0, 5, Cu Ag0, 1 and Cu Ag0, 4. Copper

material is alloyed with Mg or Ag to increase the thermal stability of the material [25]. Contact wire materials are invited to fulfil various physical properties

Table 1. Physical properties of Contact wire material (Cu Ag0, 1) [26]

Density		Electric conductivity[2)]		Thermal conductivity	Thermal Expansion [4)]	Specific heat	Elastic modulus
[g/cm^3]		[MS/m]	[%IACS] [3)]		[ppm/k]		
Conditions	20^0 C	20^0C/annealed	20^0C/annealed	20^0C	20 to 100^0C	20^0C	20^0C annealed
8.94		>58	>100	385	16.8	386	110

2) Resistivity ρ is the inverse value of conductivity, e.g. ρ = 1/58.6 =0.01724 m/MS or Ω·mm2 /m.

3) International Annealed Copper Standard: 100% IACS = 0.01724 μ Ω x m at 20°C

4) Linear coefficient of thermal expansion (CTE), as a mean value between the given temperatures

The research conducted in [27] investigated the sliding wear and corrosion resistance of train overhead contact wire. It is the experimental research with which the wear test is done through a pin on-disc tribometer machine which is designed and constructed as part of the research to simulate the contact wire and collector (contact) strips contact. Different contact wire materials were experimented (pure copper (Cu) and two copper alloys (CuAg, CuNiSiCr)).

The experiment conducted by Shibata et at al. [28], compared the wear friction properties of Copper/Carbon/Rice Brain (Cu/C/RB (Rice Brain) ceramic composite and conventional Copper/Carbon (CU/C) pantograph-catenary materials under electrical current with and without the arc-discharge. The experiment without arc discharge showed that the Cu/C/RB materials of pantograph strip sliding on the contact wire in copper presented 98% of reduction in wear rate of the pantograph material specimen and 23% reduction in that of specimen of contact wire material and 75% reduction in the friction coefficient over the CU/C conventional composite. However, under electrical current with arc-discharge, the CU/C/RB composite showed the wear resistance to arc-discharge equivalent to conventional CU/C composite [28],[29].

2.2 Environmental impact of pantograph-catenary emission particles

As environmental issues become more and more global, the role of railways as a means of transport is gaining fresh attention. In the railway field, while safer and more stable transport is accomplished by using advanced electronics technologies, it is also becoming important to develop technologies with more considerations for environment [30]. The electrified railway system is working because of the interaction between the pantograph and the catenary wire. The interface between the pantograph and the high-voltage contact wire is thus important, not just for the individual train but for the reliability of the complete OLE system. Pantograph faults are a major cause of dewirements, where snagging of the sliding carbon strip or supporting structure can lead to catastrophic damage to sections of the OLE.

As a component of current collection by friction, the pantograph contact strip is required to have good anti-friction, wear resistance and self-lubrication, as well as good conductivity and impact resistance. Since electric locomotives were put into operation, theoretical research and application study on pantograph contact strip materials have never ceased [31]. The use of carbon strip is more effective compared to other materials used before because of its properties of being consumable. This factor reduces the wear of contact wire [31]. But as result carbon strip is wearing which causes particles emission known as Black Carbon (BC) and Carbon Blacks (CBs). For the environmental and human life concern, once the emitted carbon particles mix with air, there is carbon dioxide formulation and this is among the Green House Gases (GHG) and GHG are responsible for global warming, acid rains, and climate change. Additionally, inhaling black carbon may affect human being respiratory systems and promote lung cancer. According to the study in Switzerland on the release of hazards by railway[32],[33]. Material losses from railway components due friction and wear processes are regarded as the leading cause of emissions. The contact lines account for 38 tons of materials losses per year.

2.3 Review of the existing methods of modelling overhead contact systems

The effective sliding phenomenon is affected by joule's heating effect as well the arcing which increases as the sliding speed and loads increase [34]. Back then different researches on pantograph-catenary systems were done focusing on the vibrations analysis of the rail vehicle current collection components, the aerodynamics force investigation and the design control part [35],[36]. To give a better understanding of the damage mechanism of the pantograph and catenary

contact conductor wire, various aspects like temperature variations, conductivity fluctuation and microstructure behavior of the rail vehicle power collection components are always taken into account [37]. Furthermore, the recent researches have revealed that the contact condition of the pantograph-catenary is a critical issue for the quality of current collection in electrified railways. Hence more emphasis was put on the regular monitoring of the contact condition of the pantograph- catenary system during rail vehicle operation as well as the pantograph vibration which are considered as the main criterion evaluate the dynamic performance and quality of the current collection [38]. In reference [39], the strain gauge technics was utilized to improve the measurement performance of the contact force between the pantograph and catenary system. Using a force sensor built in the strain gauge, the measured results showed that its design is worthwhile and can be used on on-line test. Therefore, the sensor was utilized as a part of a measurement system to evaluate the current collection quality more efficiently.

Various researches pointed out that wear phenomenon and contact condition of pantograph and contact wire known as the key components of the rail vehicle power supply components must be taken into consideration. The reference [40], showed the possibility of estimating the contact wire wear using the rail vehicle pantograph-catenary contact force data. Moreover, the research [41] showed that the contact wire gradient has the effect on the dynamic performance of the catenary pantograph system. It was revealed that the contact wire gradient is inevitable due to the change in clearance height of the contact wire on the bridges, tunnels and level crossing railway infrastructures. The former also showed that calculating contact loads during height transitions allows for better prediction of the sliding contact wear regime during train operation. Chu et al. [42], have studied the dynamic interaction of railway pantograph-catenary including reattachment momentum impact. The impact of the pantograph head on the contact wire at the reattachment point is considered by introducing additional velocity into the contact wire. Then, the numerical simulations were performed at high speed to analyze the pantograph-catenary interaction taking into consideration the reattachment impact phenomenon. The former showed that the perfect description of the separation and reattachment of the pantograph head and the contact wire is more important to understand the pantograph-catenary dynamics behavior. Furthermore, a procedure for wear prediction of the collector strip and the contact wire based on contact force in pantograph-catenary systems was developed in [43] and in reference [44], the wear behavior of the pantograph-

catenary sliding components was investigated in numerous past researches considering different currents and speed conditions. However, the current variation due to the change in train loading as the train moves between feeding stations has not been tackled on in the former research. Therefore, the current research considered the current changes due to train loading fluctuations and hence analyzes the impact this has on the damage condition of the contact conductor wire.

The overhead contact system modelling methods were studied by various researchers. Analytical models were performed in different studies. The researches on the dynamic interaction of the pantograph and catenary modelled the catenary system as Euler-Bernoulli beam whilst the pantograph was modelled as lumped mass systems. The interaction of the system is provided by the contact force between the two. As the pantograph is moving along the contact wire of the catenary to supply electrical current to the moving train, a moving force is taken into consideration to ensure a constant contact of the mating elements. The variation in train speed and other operating parameters may hinder a regular contact between the two component from happening all the time. Therefore, a loss of contact may be experienced. It is given as the difference in contact wire vertical deflection and the pantograph head vertical displacement. The pantograph- catenary contact model, which is depicted in Figure 5 is commonly adopted by numerous researchers [45],[42],[46] and based on it the equations of motion of the pantograph-catenary were elaborated.

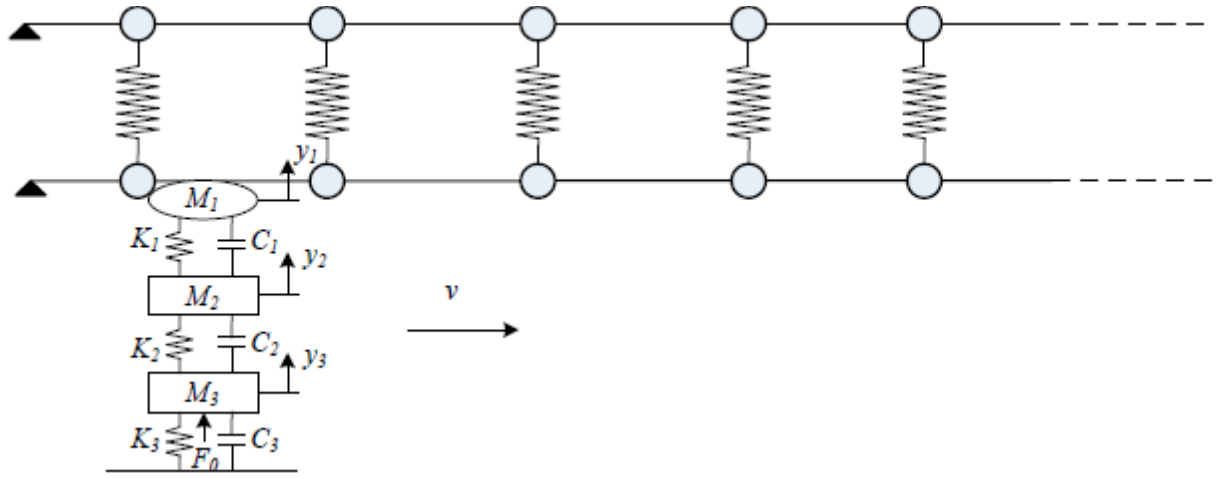

Figure 5. Pantograph-Catenary contact model[42] .

$$EI_b \frac{\partial^4 w_b}{\partial x^4}(x,t) + \rho_b \frac{\partial^2 w_b}{\partial t^2}(x,t) - T_b \frac{\partial^2 w_b}{\partial x^2}(x,t) + C_b \frac{\partial w_b}{\partial t} = \sum_{i=1}^{nd} {F_b}^i \, \delta\left(x - {x_d}^i\right)$$
$$+ \sum_{j=1}^{nr} {F_r}^j \, \delta(x - {x_r}^j) + \left(M_1 \frac{d^2 y_1}{dt^2}(t) + C_1 \left(\frac{dy_1}{dt}(t) - \frac{dy_2}{dt}(t) \right) \right) + K_1\big((y_1(t) - y_2(t)\big)vt)\delta(x - vt) \quad (1)$$

When there is a contact between the pantograph and contact wire, the interaction between the pantograph and the catenary is provided by the contact force. However, when there is a loss of contact, the motion of the pantograph and the catenary are independent of each other. This phenomenon is governed by the gap g of the contact surface and is expressed by:

$$g = w_b(vt)t - y_1(t), \quad (2)$$

where $w_b$the contact is wire vertical displacement and $y_1$is the pantograph head vertical displacement.

When g>0, the pantograph is separated from the contact wire. If g=0. The pantograph contacts with the contact wire. When the contact occurs, the motion of the contact wire is governed by the equation (2).

It is crucially important to always monitor the contact condition between the pantograph and the catenary system to ensure the stable current collection. Different modelling method are used to estimate the life condition of the catenary system including analytical method and FEM. A better selection of various modeling parameters such as train mass, train speed, pantograph up lift forces, pantograph- catenary system temperatures are is also more important. The time saving and accurate results of FEM makes it a best candidate to study the dynamic behavior of the interaction of the pantograph and catenary system. This research utilized FEM to investigate the effect of train loading fluctuation on the damage of the contact wire taking into consideration different modelling parameters train speed, train mass and pantograph strip and the contact wire temperature. The temperatures were obtained by analyzing the thermal robustness of the pantograph- catenary component by considering the train mass change due to the change in train passengers' capacity. And the latter is not considered in the past researches.

3 Materials and Methods

This section describes the methods used to model the interaction between the pantograph and contact wire. For the sake of reliable and a better investigation of the contact wire wear phenomenon, the overhead contact interaction modelling is of paramount importance. Throughout this section, the FEM method which is commonly used to model the overhead system interaction is discussed, different modelling input parameters are listed and railway power flow analysis is performed to know the effect of passengers' load fluctuation of the rail vehicle power consumption hence conduct thermal behavior analysis of the interaction between the current conducting sliding components. Moreover, this section presents an overview of contact wire wear model analysis. Archard wear model commonly used to estimate the adhesion wear phenomenon experienced by two sliding components is tackled on in this section. Furthermore, a 3D model design of both the pantograph and contact wire are designed using ABAQUS UNIFIED FEM software package. Finally a dynamic simulation is carried out to investigate the dynamic behavior of the pantograph-catenary interaction during rail vehicle operation.

3.1 Overhead contact system interaction modelling using FEM

To draw a precise and reliable picture of the contact conductor wear, overhead contact system interaction modelling is required. This gives the dynamic behavior of the interacting components (i.e. pantograph strip and contact wire). Various modelling methods exist for this dynamic behavior analysis including analytical and numerical models. Because of the complexity of many parameters that take role into pantograph catenary system interaction behavior such as contact interaction, friction, temperature effects, current flow, vibrations, wire oscillations, and the nonlinear behavior of the system interaction, FEM is the best choice to handle this modeling. Therefore, for this research explicit dynamic finite element method is adopted using ABAQUS UNIFIED FEA software.

The current research estimates the influence of rail vehicle loads variation on the change of rail vehicle power consumption, which results into change in thermal behavior of the sliding pair components, which, in-turn, influences the wear of the contact wire. Explicit dynamic FEM tool, ABAQUS UNIFIED FEM software package, is used. MATLAB software is also used to solve the electric circuit thermal equation of the sliding elements (i.e. contact strip and contact wire). The heat losses at various energy consumption or train loadings are inputs to a thermal equation. The

latter gives the inputs parameters such as predefined temperatures for FEM model simulation. The other modeling parameters are collected from AALRTS as the case of study of the current research as well as from the reviewed literature. Moreover, the following sections detail the methods described in above paragraphs.

3.2 Theoretical calculations: Overhead contact system interaction

This study was conducted based on the parameters collected at Addis Ababa Light Rail Transit Systems (AA-LRTS) as well as from the reviewed literatures. These include the major technical dimensions of AA-LRTS vehicle (i.e. N-S line), Main parameters for AA-LRTS track (Rail), operational performance for AA-LRTS vehicles, Electric parameters of the train, Rail infrastructure Electrical Parameters and the Rail vehicle weight parameters including the passenger capacity as presented in Tables 2 through 7.

Table 2. Major technical dimensions of AA-LRT vehicle (N-S line)

Descriptions	Dimensions
Vehicle length	$\leq 28400\ mm$
Vehicle width	$2650\ mm$
Vehicle height(from track top to vehicle top ,Pantograph height excluded)	$\leq 3700\ mm$
Wheel base	$1900\ mm$ (power bogie) $1600\ mm$ (driven bogie)
Vehicle body length, Powered module(excluding couplers and articulations	$\leq 11780\ mm$
Vehicle length, Trailer module(excluding articulation)	$3600\ mm$
Distance between High-Floor area and Track top	$865\ mm$ (Power module in vehicle body)

	365 mm (Trailer module in the vehicle body)
Distance between Low -floor area and track top	365 mm(Power module in vehicle body) 365 mm(Trailer module in vehicle body)
Motor wheel diameter	660 mm(New) 640 mm (Half-worn)
Driven wheel diameter	600 mm(New) 580 mm(Half-worn)
Side doors for passenger compartments(4 pairs electric sliding doors per side)	$\leq 1250X1850\ mm$
Clear opening of passenger doors(width $\boldsymbol{X}$ height)	$\leq 1250X1850\ mm$

Table 3. Main parameters for AA-LRT track (Rail)

Descriptions	**Dimensions**
Track Gauge	1435 mm
Minimum curve radius	50 m(for main lines) 30 m(for parking yard)
Minimum vertical radius	100 m

Maximum Gradient	50‰
Track type	50 kg/m

Table 4.Operational performance for AA-LRT vehicles

Description of items	**Operational performance(value)**
Dead weight of the vehicle	43 t
Weight Per axle	$\leq$ 11 t
Maximum operation speed	70 km/h
Average travelling speed	$\geq$ 20 km/h
Average acceleration for start-up	1 m/s^2
Average Deceleration for braking: from 70km/h to stop	$\geq$ 1 m/s^2 (normal braking with rated load, including control response time) $\geq$ 1.5 m/s^2 (Emergency braking with rated load, including control response time)
Number axles on the rail vehicle(uncoupled)	6 (4 driving axles and 2driven axles)
Number of seats in one vehicle	64
Rate passengers per rail vehicle	286 persons + standing persons: *6 persons/m^2*
Average weight of each passenger(Assumption)	60 kg
Average Dwelling time	30 s

Table 5. Electric parameters of the train [47],[2]

Parameter	Value
Voltage Minimal voltage Nominal Voltage Maximum voltage	 1000 V 1500 V 1800 V
Powertrain efficiency In traction In braking	 0.9 0.85
Traction motor used(4 motors)	ϕac Squirrel-cage induction motors with $\eta \geq 97\%$

Table 6. Rail infrastructure Electrical Parameters [47],[2]

Parameter	**Value**
DC network Nominal voltage Resistance of the catenary Resistance of two rails in parallel	 $1500\,V/750V$ $0.021\ \Omega/km$ $0.015\ \Omega/km$
Traction substation Internal Resistance No-load voltage	 $0.02\ \Omega$ $1500\ /750\ V$
Substation inverter type	VVVF

Table 7. Rail vehicle weight at AA-LRT.

Load	**Carbody dead weight(t)**	**Passengers' weights(t)**	**Total weights(t)**
Empty vehicle	43	0	43
Half seating capacity	43	8.58	51.58
Seating capacity	43	17.16	60.16
Overload capacity	43	21.42	64.42

3.2.1 Railway power flow analysis using simplified power network circuit

The traction power network adopted in this research comprises of feeding stations, contact line (catenary), return rails (return tracks) and one train. Figure 6 represents a simple power network circuit which is utilized throughout this research. The resistance of the contact line and track rails are determined by the length of network and the resistivity of both contact line and the track rails. When the train moves, the resistance of the network changes with the train locations. The voltage and the current drawn by the train varies with the train locations. The distance between two substations is utilized to study the effect of train overloading on the current fluctuations, which results in temperature change for both the pantograph contact strip and contact conductor, which, in-turn, induces the wear of both the contact conductor and the pantograph strip. The literature indicates that the average interval between two adjacent feeding substations for a 750 Volts DC railroad may vary between 4 to 6 km [47]. AA-LRTS feeding substations distances is 2km

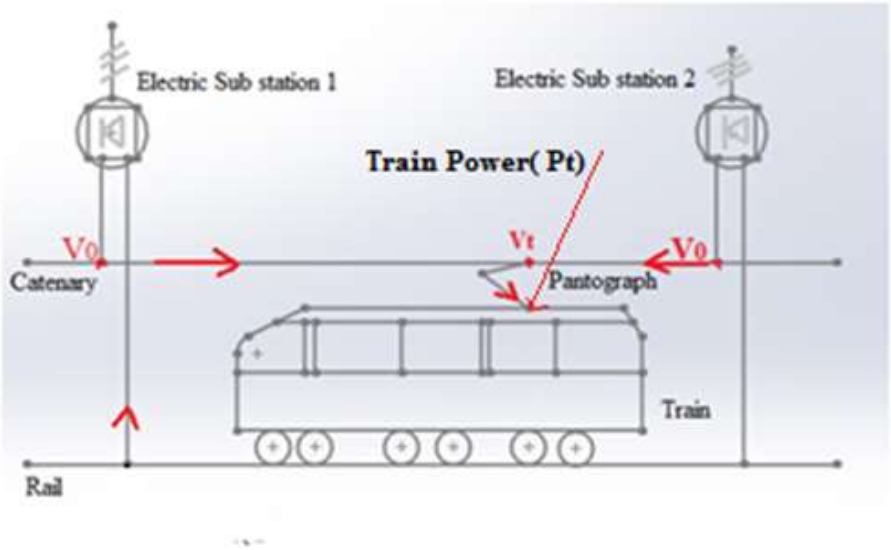

Figure 6. Simple power network circuit with train positioned between 2 power feeding stations.

3.2.2 Estimation of power consumed by a suburban electrical Railway

The power consumed by the electric railway is given by the product of the available tractive effort developed by the traction unit of the train and the speed of the train divided by efficiency that combines mechanical power transmission, power conversion by DC motors and electrical power transmission from the catenary to the motors:

$$P_t = \frac{F_t \times V}{\eta} \tag{3}$$

where F_t,V and η are respectively the tractive effort in N, speed of the train in m/s and overall efficiency of the power transmission from the catenary to the driving wheels.

The tractive effort (F_t) is the force necessary to move a train and its trailers provided the running resistances are overcome. For a train to start moving the tractive effort should be less or equal the train hauling capacity.

$$F_t \leq \mu \times M \times g \tag{4}$$

where F_t, μ, $M$and g respectively are the tractive effort, dynamic adhesion coefficient, total mass of the train including the train dead mass and the passengers capacity and the gravitational acceleration.

The dynamic adhesion coefficient is obtained by considering the change in speed of the rail vehicle. The adhesion coefficient is estimated in literature by different countries railway system and the experiment adapted in this research is the one developed by Chinese railway for the electric locomotives [48] (See Equation (5). Moreover, other literatures showed that value of the dynamic adhesion coefficient may also be obtained by considering the change of the static adhesion coefficient μ_0 with respect to train's speed. Therefore, μ may also be calculated using the Equation (6).

$$\mu = 0.24\frac{12}{100 + 8V}, \tag{5}$$

$$\mu = \frac{\mu_0}{1 + 0.01V}, \tag{6}$$

where V is the train speed.

3.2.3 Power output of the traction motors

It is defined as the total power consumed by the train traction motors. It is found by dividing the power output from the driving axles with the combined efficiency of the transmission gear and the motor gear.

$$Power\ consumed\ by\ traction\ motots = \frac{Power\ output\ of\ the\ driving\ axles}{\eta\ of\ transmission\ grear * \eta\ of\ motor\ gear}$$

$$\therefore P_{motor\ cons} = \frac{F_t \times V}{\eta}\ [watt\ or\ kW]$$

η is the combined efficiency of the transmission gear and the traction motors gears.

3.2.4 Traction motors specifications

It is paramount importance to improve the efficiency of traction motors to save energy in electric trains. Moreover, improving the efficiency push in need of designing totally enclosed traction motors that require less maintenance [49]. The novel emerging issue of increasing the energy efficiency in DC railway systems is also in the context of global concern in reducing CO_2 emission by cutting down the energy consumption and energy loss [50]. Table 8 details the key specifications of tractions motors commonly found in rail way commuter train application [51] [13,14]. Which behave well when it comes to energy efficiency.

Table 8. Specifications of traction motors used in commuter train.

	Motor type	Permanent magnet synchronous motors		Induction motors
	Cooling system	Totally-enclosed		Self-ventilated
Rating	Class	Continuous	1hour	1hour
	Output power	140 kW	200 kW	200 Kw
	Voltage	1000 V	1100 V	1100 V
	Current	108 A	148 A	130 A
	Rotational speed	2550 min^{-1}	2550 min^{-1}	2535 min^{-1}

	Efficiency	97%	97%	92%
	Lubricant	Grease		Grease
	Mass	570 kg		595 kg

3.2.5 Power flow simulation parameters

The current flow and the contact conductor temperature rise due currents are solved sequentially for the case of AALRTS. The AALRTS line is 31.6 km with 39 passenger stations, 41 vehicles and 20 substations. The interval between two adjacent feeding stations is taken to be 2000 m. The rated power for the traction substation is set to 3 MW with the power traction type of 750 KW MCT (Motor Controlled Thyristor. The rolling stock uses DC750V over-head contact wire power system and the top speed is set to be 70 km/h.

3.2.6 Calculation of current flow

The current flow to the train is determined by solving the power flow equation of the railway system. Figure 7 shows the train current flow schematic. Equation (7) represents the current flow equation, Equation (8) represents the power consumed by the train whilst Equation (9) stands for the heat power losses due to Joule's effect.

$$I_1 = \frac{V_o - V_t}{R_c}, I_2 = \frac{V_o - V_t}{R_r}, I_3 = I_1 + I_2, P_t = V_t I_3 \tag{7}$$

$$P_t = V_t \left(\frac{V_o - V_t}{R_c} + \frac{V_o - V_t}{R_r} \right) \tag{8}$$

$$P_1 + P_2 = R_c I_1^2 + R_r I_2^2 \tag{9}$$

where V_o is the feeding substation voltage in V , P_t is the train power consumption in (Watt). $R_c \; and \; R_{r,}$ are the catenary and rail resistances in Ω/km , I_3 is the current drawn by the train in A and V_t is the train voltage in V.

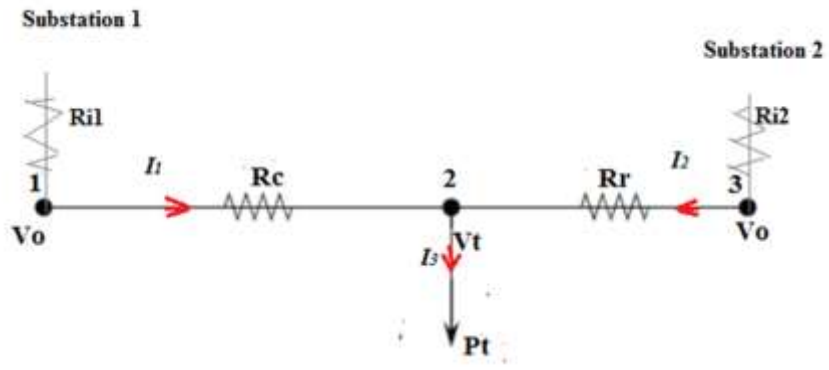

Figure 7. Train current flow schematics.

3.2.7 Calculation of contact wire temperature

Using the energy balance theory, the temperature behavior of the contact wire was estimated when a train is moving between 2 feeding stations. Equation (10) demonstrates the energy balance theory. E_{in}, represents the power input to the conductor, which is equal to the heat generated due to Joule's effect or energy being generated, E_{out} represents the total energy loss, which is the summation of energy loss due to convection, energy loss due to conduction and energy loss due to radiation and E_{stored} represents the energy stored in the conductor.

$$E_{in} - E_{out} = E_{stored} \tag{10}$$

$$E_{out}=E_{out}(Conduction)+ E_{out}(convection) + E_{out}(Radiation) \tag{11}$$

From Equation (11), $E_{out}(Conduction)$ is neglected since the contact conductor may be long and is not connected to any massive heat sinks. Therefore the Equation (11) may be written as:

$$E_{out}=E_{out}(convection) + E_{out}(Radiation) \tag{12}$$

$$E_{stored}(Energy\ being\ stored) = E_{in} - E_{out}(Convection) - E_{out}(Radiation) = mC_p(T_n - T_{n-1}) \tag{13}$$

- **Energy loss due to convection**

Using Newton's law of cooling, the energy loss due to convection is found as follows

$$E_{out}(convection) = hA(T_{n-1} - T_0)dt \tag{14}$$

where $h, A, T_{n-1,} T_0 \; and \; dt$ are, the convective heat coefficient, the area of contact wire, temperature of the previous data, initial temperature and time increment (allows calculating the wire temperature as time continues) respectively.

- **Energy loss due to radiation**

$$E_{out}(Radiation) = \varepsilon A\sigma((T_{n-1})^4 - (T_0)^4)dt \tag{15}$$

where $\varepsilon \; and \; \sigma$ are the emissivity and the Stefan Boltzmann constant (in$\frac{W}{m^2K}$) respectively

- **Energy being generated**

$$E_{in} = (R_c I_1^2 + R_r I_2^2 \;)dt \tag{16}$$

where, I, R are the current input to the contact conductor and the resistance of the contact conductor respectively.

- **Temperature of the contact conductor**

Using Equation (13) the temperature of the contact conductor is obtained.

$$T_n = T_{n-1} + \left(\frac{E_{in} - E_{nout}(convecion) - E_{out}(Radiation)}{mC_p}\right) \tag{17}$$

By plugging Equations (14), (15) and (16) into Equation (17), Equation (17) can be rewritten as follows:

$$T_n = T_{n-1} + \left(\frac{= (R_c I_1^2 + R_r I_2^2 \;)dt - hA(T_{n-1} - T_0)dt - \varepsilon A\sigma((T_{n-1})^4 - (T_0)^4)dt}{mC_p}\right) \tag{18}$$

Note:

- All energies are estimated in joules.
- At time equal to zero, the $E_{out}convection)$ and $E_{out}\; Radiation)$ are zero since $T_n = T_0$

- At time equal to zero, E_{in} is not Zero
- Temperature of the contact wire varies as time continues or a train is moving.

3.3 Wear model flow chart

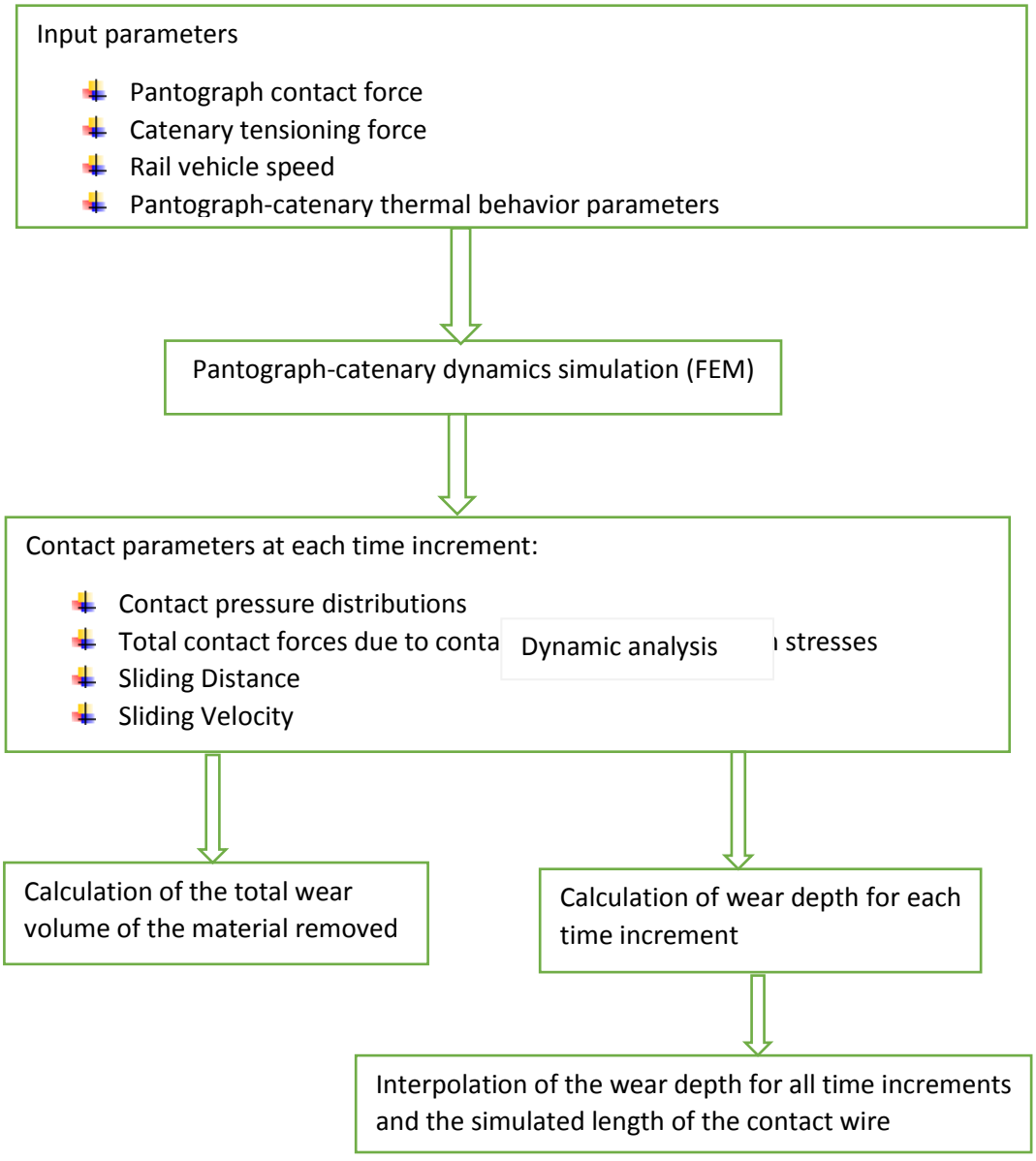

Figure 8. Procedures to evaluate the contact wire wear.

3.4 Archard wear model theory

Archard's wear model is commonly used in tribology to compute wear due to sliding. The model was developed by Archard and Hirst [52],[53] in relation to the adhesive wear. It is generally termed Archard Equation and it is demonstrated as follows:

$$V_w = K \times \frac{F \times S}{H} \tag{19}$$

where V_w is the volume of worn material(mm^3), F is the normal formal force over the contact area (N), K is the wear coefficient, S is the sliding distance of the material under study (mm), and H is the hardness of the material under study$\left(\frac{N}{mm^2}\ or\ Mpa\right)$.

The value of the wear coefficient K is usually obtained from the experiment data, using twin disc and pin on disc component results and it depends on the types of material under sliding contact. The research conducted in [54] shows that K can vary enormously; situations of very mild wear generates value of less than $10^{-9}\ \frac{mm^3}{Nm}$ while values of $10^{-4}\ \frac{mm^3}{Nm}$ or more would generally be considered unacceptably severe for most tribological situations. Moreover, the experiment carried by Archard[52] on the wear behavior of various combination of materials postulate that the value of K for the copper alloy materials is equal to $6 * 10^{-4}$ for the copper alloy materials of around $950\ MPa$ of hardness and it is estimated to be $1.7 * 10^{-4}$ for the copper alloy materials of around $700\ MPa$.

As the current research is trying to investigate the influence of the train overloading on the thermal behavior of the pantograph-catenary interaction, particularly the wear of the contact conductor, the value of K equals to $1.7 * 10^{-4}$ is selected provided the material of the contact wire under study is made in copper alloy [55],[56] and K is in good agreement of coefficient friction calculated using data from [24] showing the value of K of around $1.75 * 10^{-4}$.

Furthermore, in the relevance of the research under study, the following equations (20) and (21) elucidate the expression which are going to be utilized to calculate the volume of material removed for the contact conductor wear as well as the wear depth.

$$V_{w_{tot}} = \frac{1}{H}\sum K S_i F_i \tag{20}$$

$$D = K\frac{S_i P_i}{H} \tag{21}$$

where $V_{w_{tot}}$ is the total volume of the material removed(mm^3), K is the wear coefficient, S_i is the sliding distance at each time increment(mm), F_i is the normal contact force at each time increment, H is the hardness of the material under study (MPa), D is the wear depth(mm) and P_i is the contact pressure at each time increment(MPa).

3.5 Numerical modelling method

This section gives a clear image of the modelling techniques undertaken throughout this research. The modeling parameters are demonstrated such as the input data, the material properties as well as the pantograph and contact wire design drawings are postulated.

3.5.1 Material data of overhead contact systems and other technical specification of contact wire

The contact wire design utilized in this research is for electrified railway overhead contact systems(OCS) of Ethiopian Light Rail Transit project and it is based on Chinese Railway standards [57]. Figure 9 and Table 8 respectively represent the srtucture and sectional dimension of contact wires of Addis Ababa Light Rail Transit.

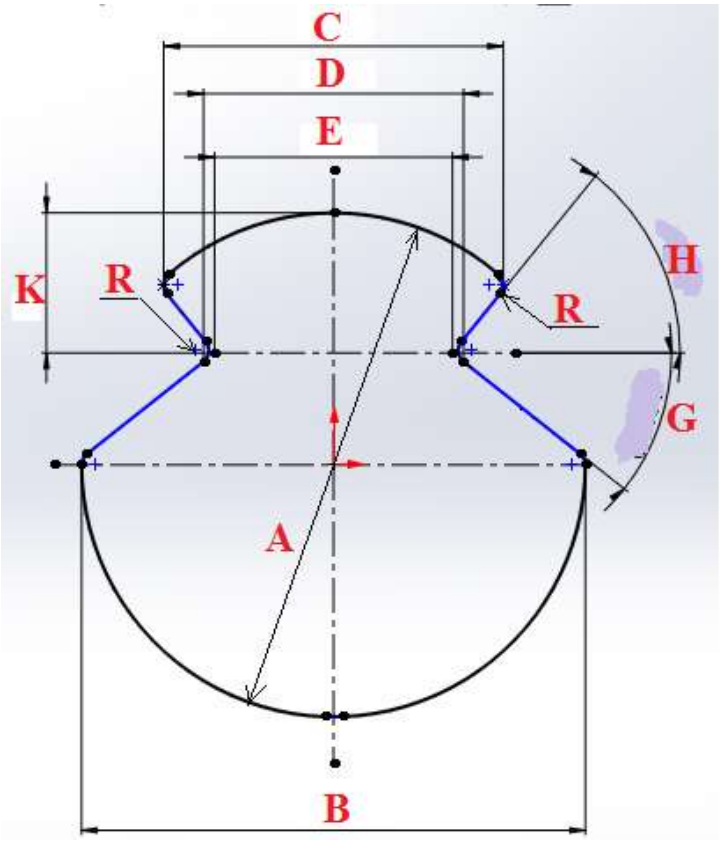

Figure 9. Section structure of contact wire used at AA-Railway.

Table 9. Design dimensions of contact wire used at AA-LRT railway.

Size Type	A(mm) ±1%	B(mm) ±2%	C(mm) ±2%	D(mm) +4% -2%	E (mm)	K (mm)	R (mm)	G(^{0}) ±1^0	H(^{0}) ±1^0
150mm^2 silver-copper alloy contact wire	14.40	14.40	9.71	7.24	6.80	4.00	0.40	27	51
120mm^2 silver-copper alloy contact wire	12.90	12.90	9.76	7.24	6.80	4.35	0.40	27	51

3.5.2 Material properties of AA-LRTS overhead contact systems

The contact wire FE model was assumed to be cylindrical with grooves to hold the droppers connecting the contact wire to messenger wire to make a complete system of railway overhead catenary.The model of the contact wire is designed in solidworks and then after imported in ABAQUS.The material properties of the overhead contact system used in this research is of Addis Ababa Light Rail Transit(AA-LRT). AA-LRT project is of chinese railway standards. Therefore, chinese suburban railway materilas are taken into considerations thropught the research under study.The materials properties of the overhead catenary system utilized are shown in Table 9.

Table 10. Material properties of AA-LRT overhead contact systems.

Material	**Sliver-copper alloy(CuAg)**
Density	$1.04E^{-6}\ kg/m^3$
Modulus of Elasticity	$120E^3 MPa$
Poison ratio	0.3
Tensioning force	$12\ KN$
Conductivity	$4.2\ W.cm/cm^2$℃
Specific Heat	$0.245\ j/g$℃
Heat expansion coefficient	$1.7E^{-6}cm/cm$℃

3.6 Pantograph and contact wire model design

3.6.1 Contact wire 3D model

To build a 3D model, the aforementioned AALRT contact wire structure and dimenstions were adopted.Throught this research, contact wire for main lines and access lines is considererd. It is of a design dimater 14.5 mm and of Silver-copper alloy material.Solid work softaware was used to generate a 3D model. The Soldworks model is imported in ABAQUS software package in order to perform the FE analysis of the pantograph-catenary interaction.It is obvious to note that the catenary system of 3000 mm length is selected so as to limit the number of elements and reduce the computational time of the the Finite Element Analyis (FEA). Figure 10 represents contact wire used at AA-LRTS a) depicts sectional dimensions of the contact wire and b) depicts 3D schematic of the contact wire.

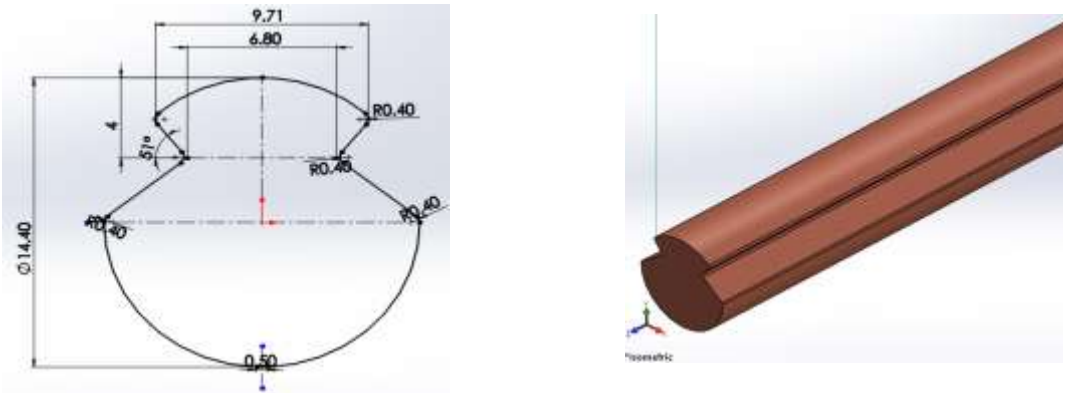

(a) (b)

Figure 10. Contact wire design used at AA-LRTs. (a) Sectional dimension of the contact wire; (b) 3D schematics of the contact wire.

3.6.2 Pantograph 3D model

The description of the pantograph model is as important as compared to the catenary. The pantograph 3D model is described using solid works and ABAQUS software packages. The modeling parameters are of AALRTS pantograph design presented in [58]. The model consists of upper frame, pan collector (2contact strips), springs and dampers. The pantograph contact strip is of metalized carbon, the upper frame is of steel material. The springs and dam (b) nect the pantograph with railway vehicle. The flexible upper frame of the pantograph and individual springs on each side frame result in different degrees of freedom of the pantograph mechanism. Three degrees of freedom are necessary for describing the translational motion of the upper frame and the pan collector assembly. The other 3 degrees of freedom are required in order to generate the rotation motions of pantograph frame and the pan head collector about X, Y, Z coordinates. The non-linearity of the pantograph dampers must also be taken into account when building the model. Moreover, the gravitational loading of the pantograph assembly is taken into consideration. However, the aerodynamic loading effect on the pantograph is neglected when establishing the model.

The pantograph used in the current research was sampled from the AA-LRTS pantograph design presented in [56]. Solid works software was used to produce a model depicted in Figure 11.(a), (b) and (c) while (d) is an import of (b) from solidi works to ABAQUS to apply the springs and damping components. Moreover, the pantograph material properties are shown in Table 11.

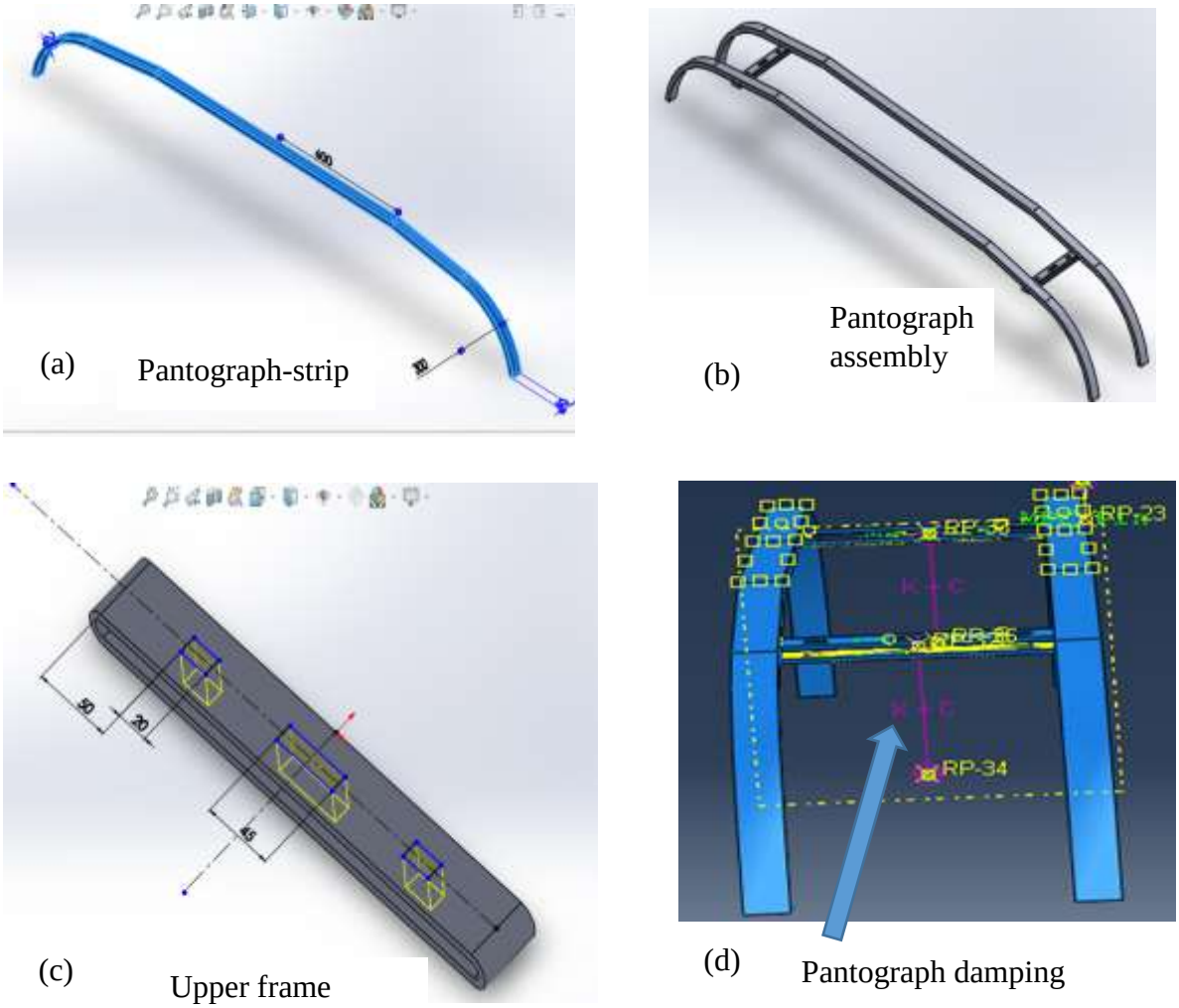

Figure 11. 3D model of pantograph. The dimensions and design parameters are of a typical pantograph head used at AA-LRTS.

Table 11. Material properties of Pantograph used at AA-LRT (i.e. Pantograph strip and frame).

Pantograph carbon strip	
Material	**Metalized carbon**
Density	$1.68E^{-6}\ kg/m^3$
Modulus of Elasticity	$98.7E^3 MPa$
Poison ratio	0.34
Conductivity	$4.2\ W.cm/cm^2$℃
Specific Heat	$0.71j/g$℃
Heat expension coefficient	$4E^{-6}cm/cm$℃
Pantograph frame	
Material	Steel
Density	$7.8E^{-9}\ kg/m^3$
Modulus of Elasticity	$210E^3 MPa$
Poison ratio	0.3
Conductivity	$0.45\ Wcm/cm^2$℃
Specific Heat	$0.71j/g$℃
Heat expension coefficient	$1.3E^{-6}cm/cm$℃

3.6.3 Pantograph-catenary interaction model

As of today electrified railway uses overhead catenary system to supply current to the moving train. The immense technology is the contact strip of the pantograph sliding against the contact wire of the catenary for current collection Figure 12. The correct pantograph-catenary dynamics is of paramount importance for the current collection quality. It is unlikely that designed model used in this research will provide a reasonable approximation of a true relationship of pantograph-catenary interaction of various railway design but it works well for the catenary design selection adopted within this research. Currently, the advance in computer technologies paves the way to studying the dynamic behavior of the overhead line/pantograph system via finite element and numerical simulations technique. Numerical simulations of the dynamics of the pantograph and catenary are based on mathematical modelling [59]. The significance of the simulation calculation is linked to the conformity of the simulation input parameters up on which the realistic model is

based. The design parameters used in this research are therefore of Addis Ababa Light Rail Transit. Once the simulation model works quite well, it is utilized to investigate the wear of the contact wire during train operation and also investigate the effects of different parameter change (e.g. train speed, amount of current drawn due train loading fluctuations, and number of pantograph passes) on the wear of the contact wire, hence predict its life span and strategize its maintenance. The numerical simulation has the advantage of being cost effective and of having low degree of time consumption much better than conducting field measurements and indoor experiments.

To simulate the interaction of pantograph-catenary, the pantograph will operate at static lift force of 100 N [58]. The tensioning force of 12 KN [57] is also applied for the contact wire. However, the pre-sage of contact wire is not taken into account during the simulation.

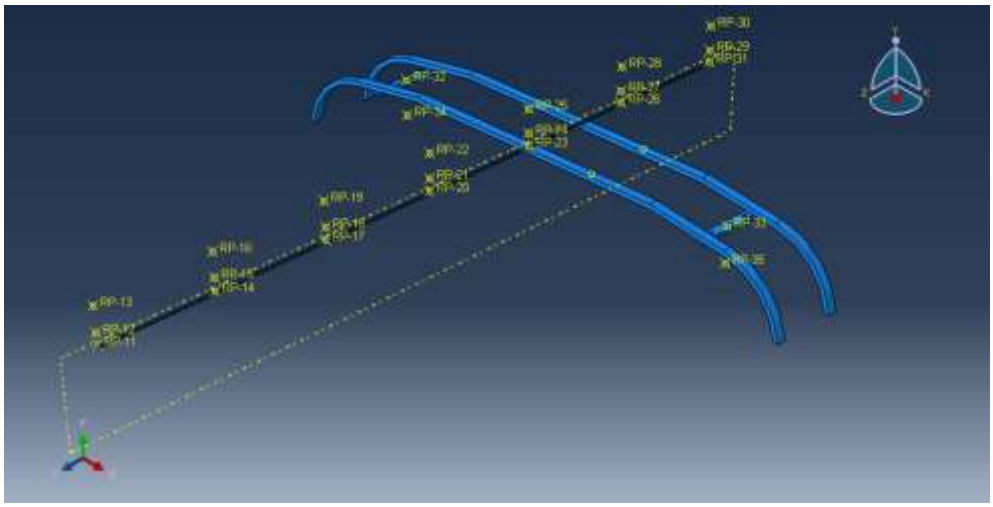

Figure 12. Pantograph-Catenary interaction model. Penalty function method is utilized to provide a good interaction of the pantograph-catenary system.

3.6.4 Pantograph-catenary dynamic simulation using FEM

The analysis was executed in 3 steps (i.e. Initial step, Step-1 and Step-2). Boundary conditions are applied in different steps and are propagated or computed from one step to the other. Static analysis was executed in the single step called Step-1 with the time step of 0.01 $seconds$. The load is applied in this step and the ramp amplitude was used throughout the loading process. The dynamic temperature-displacement explicit analysis is executed in Step-2. The former took into account the displacement of the interaction component and the thermal robustness of the components due to joule's heating effects. Figure 13 shows the components of the interaction of the pantograph-

catenary (i.e. pantograph strip, pantograph frame, contact conductor and dropper represented by springs and damper components). Table 1 and Table 2 respectively show the materials properties of pantograph and catenary systems used at AA-LRTS and they are adopted materials in undertaken pantograph –catenary dynamic FEM model.

The next section describes the boundary conditions applied, the loading application as a well the sequence of the FEM analysis with respect to temperatures.

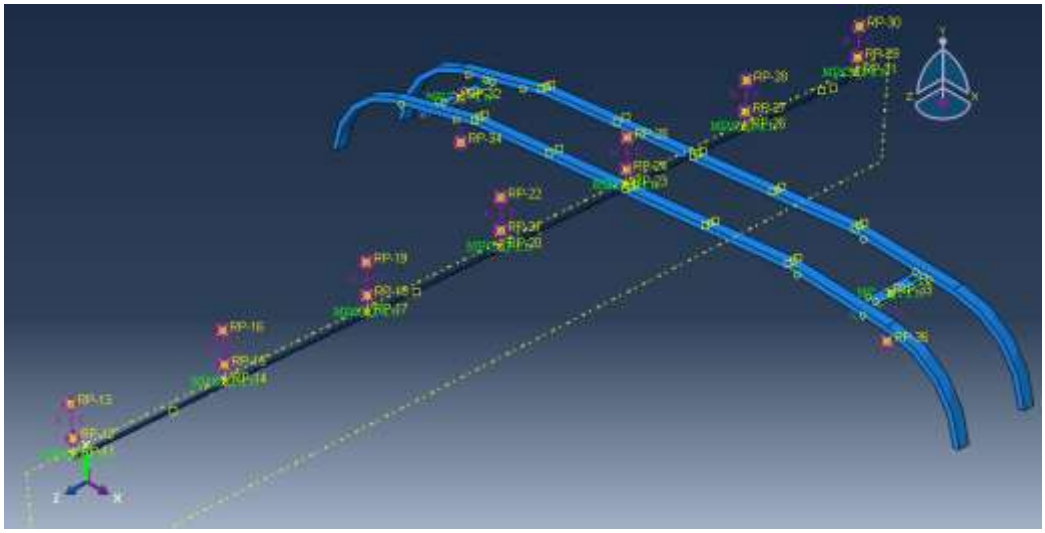

Figure 13. Pantograph-Catenary interaction components. The messenger wire is represented by point masses while the droppers are designed as spring-damper elements.

3.6.5 Applied boundary conditions

- The contact conductor is fixed in initial step and it is allowed to be free in x and z direction during the subsequent steps when the pantograph uplift force, the extension on the catenary and the rail vehicle velocity are applied. The pantograph uplift force of 100 N, the force due to gravity from the contact wire weight, the contact wire tension force of 12KN and the vehicle speed of 70 km/h are considered during the current research.
- The droppers are constrained so that only the deformation in y-axis is ensured and are also allowed to move with the contact wire along its designed length of 2500 mm.
- The pantograph lower frame fixing it on the roof of the rail vehicle is encastred during initial step.

- The pantograph upper frame together with two pantograph-carbon strips are constrained to only have one degree of freedom (DoF) in y-axis during the Step-1 and propagated throughout the subsequent steps.
- A tie constrain was defined between the pantograph frame and the pantograph contact strip. Multiple-points constraints together with pin were defined to link different droppers with the contact conductor wire and be able to move with it once it is sliding on the pantograph. The lumped mass-spring-dashpot droppers are adopted to link the contact wire with the messenger wire and they are constrained to only undergo flexibility in y-axis direction. Furthermore, the droppers are modelled as a combination of springs and dashpots (damping effect)

3.6.6 Meshing manager

For the sake of the reasonable computation time and the accuracy of the simulation results, a suitable meshing type, messing size and the assigned element type are of paramount importance. The coupled-temperature displacement element (C3D8T, an 8-node thermally coupled brick, trilinear displacement and temperature) was used to study the thermal behavior of the contact conductor when it is sliding on the pantograph contact strip in the current research. The meshing size was selected according to the length of the contact conductor modelled and the speed of the rail vehicle. It is worth to note that the contact conductor was modelled as a beam element with length of 3,000 mm. However, the pantograph sliding distance on the contact conductor was taken to be 2,500 mm. With the rail vehicle speed of 15000 mm/s (54 km/h), a running period of 0.166 seconds is generated, which results into running frequency of around 6 Hz. To portray a perfect scenario of sliding phenomenon between the contact conductor and the pantograph-strip, the number of frames to cover on the whole running distance should be taken into consideration. Therefore, 600 frames were utilized in the current model and to cover a single frame, a time period equal to 2.7 *10^-4 seconds is needed (i.e. Total time period/Number of frames). The latter has generated the element size equivalent to 4.15 mm within the speed of 54 km/hr. Moreover, imbedding on the aforementioned details a comparison is made between the meshing size of 4 mm which was utilized on the contact conductor –pantograph interaction and the element size. Therefore, it is clear to observe that element size is in good agreement with the mesh size. Figure 14 represents the pantograph-catenary interaction meshed model.

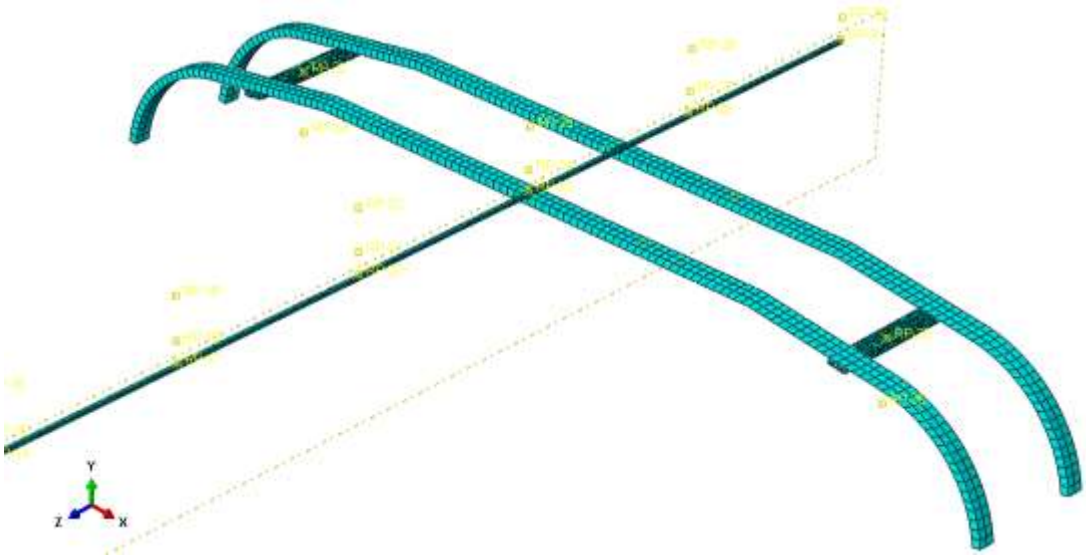

Figure 14. Meshed pantograph- catenary assembly model.

4 Results

4.1 Power flow analysis results

The power flow analysis is a crucial part of the current research. The power flow portrays the rail vehicle power consumption phenomenon which in turn shows the effects of power fluctuations on the thermal behavior of the pantograph-catenary interacting components. The rail vehicle power consumption is affected by different existing factors such as the driving speed, the conditions of the track road, the variation of rail vehicle passenger's capacity and so forth. The passengers' capacity variation factor was considered in the current research to study the effects of passengers' capacity fluctuation on the power consumed by a rail vehicle, hence investigate the effects of the power consumption of the change of thermal behavior on the pantograph-catenary dynamic and further study the effect of the thermal behavior change on the wearing condition of the contact wire. Table 4 represents the passenger capacities used at AA-LRTS and a passenger average mass of 60 kg was considered in this research.

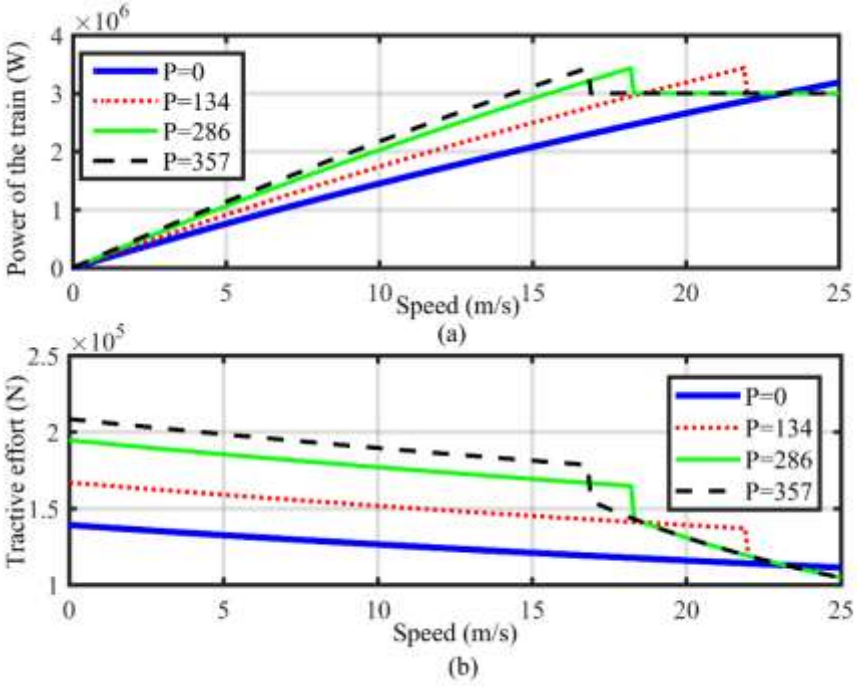

Figure 15. Vehicle power consumption alongside with variation in rail vehicle tractive effort against vehicle speed at different passengers' capacity; (a) train power variation with passenger's capacity, (b) Train Tractive effort variation with passenger's capacity. P represent the number of passengers with an average weight of each passenger taken as 60 kg.

Figure 15 demonstrates the variation of the power consumed by the train alongside with rail vehicle tractive effort variation as the number of passengers change. Using different parameters of AA-LRTS vehicle including the vehicle resistances, the loaded train total mass as the well as the rail vehicle speed, it is clear for Figure 15 that the power consumed by the rail vehicle as well as maximum tractive effort increase with the increase in number of vehicle passengers for a given speed. Furthermore, the train tractive effort changes with the variation in the adhesion coefficient as the train speed increases (see Equation (3)) and it must be less than the train hauling capacity.

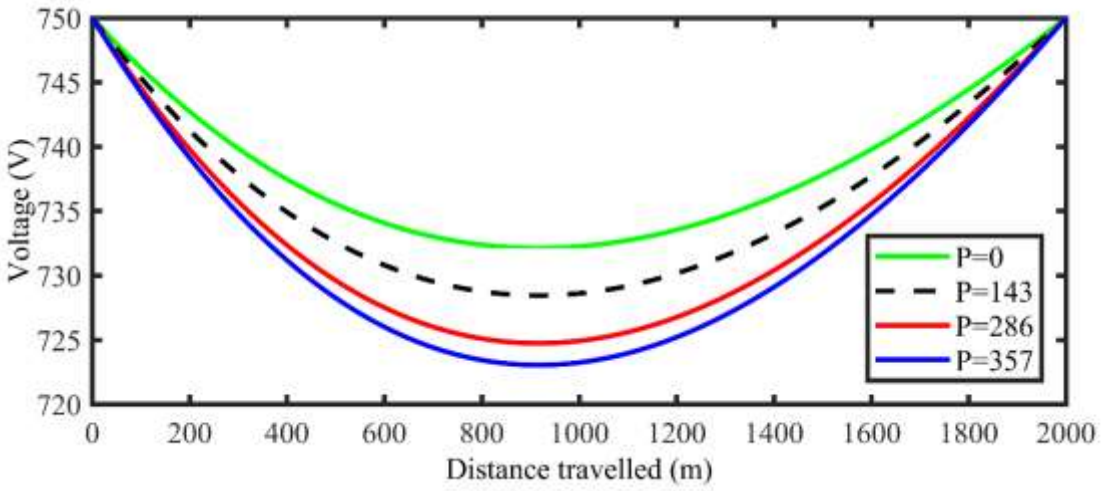

Figure 16. Train voltage against distance travelled between two feeding stations considering various train passengers' capacity.

The electrical train draws voltage from feeding substations via the pantograph-catenary systems. The resistance of the catenary and the resistance of two rail in parallel change as the train move from one feeding substation to another. The resistance change is the source of the voltage drop which results in thermal behavior of the interacting components as a result of Joule's heating effects. As it easy to observe for Figure 16 the increase in train mass due to the increase in passengers' capacity causes the increase in voltage drops which results in dramatic increase in electrical current consumed by a train once it is moving between two adjacent feeding stations. Equations (7) and (8) were used to calculate the voltage drops and the current consumed by an electrically powered train at AALRTS. Figure 17 shows the variation of train electrical currents as the number of passengers change. The distance between two adjacent substations were taken to

be 2 km as from AA-LRTS operating parameters. The driving speed of 70 km/h was used in the current research and this is the roof speed of the AA-LRTS trains.

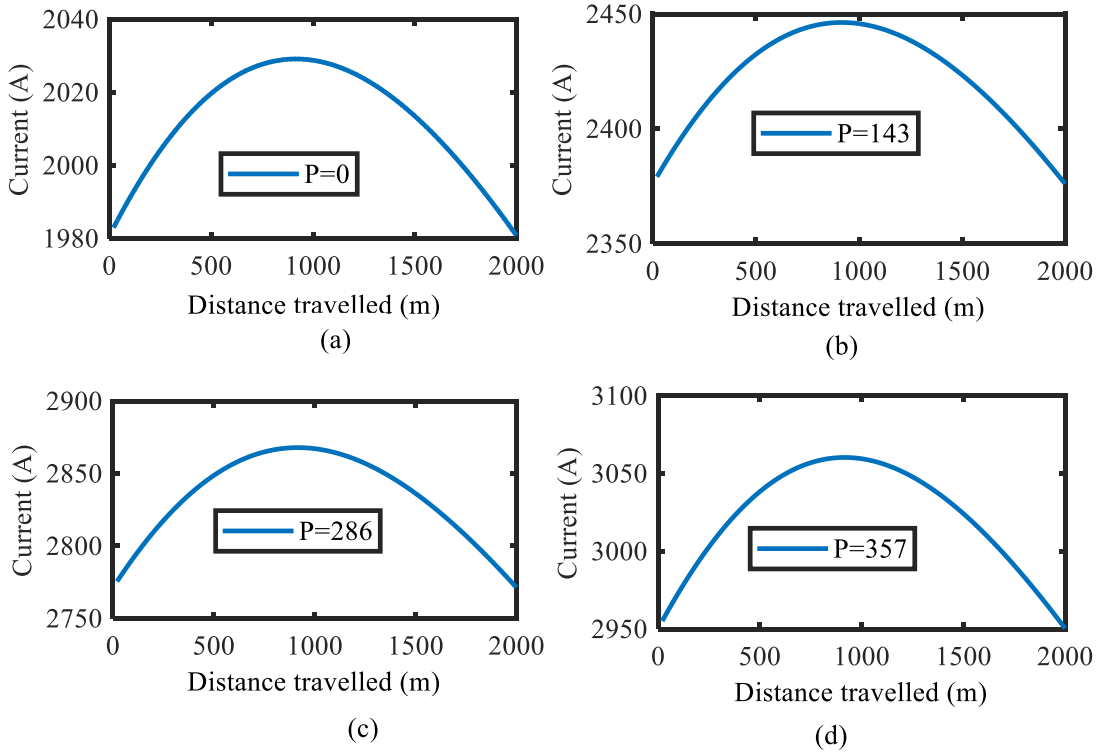

Figure 17. Currents with different passenger's capacity as the train move between two adjacent substations.(a) Current variation at Empty train (0 Passengers);(b)Current variation half capacity (143 passengers); (c) Current variation at full capacity (286 passengers);(d) Current variation at overload capacity (357 passengers).

4.2 Dynamic analysis results of the pantograph-catenary interaction

The parameters used in the analysis are of AA-LRT and the contact between the pantograph and the contact wire reflects the hertz contact theory. A half-sphere contact patch was considered in the longitudinal direction. Basing the hertz contact theory and the penalty contact method the contact patch dimension were found to be, a=6 and b=4. The pantograph-catenary dynamics contact results were obtained at exactly the contact patch for each frame during the analysis (i.e. contact pressures, normal contact forces, slip velocities, sliding distance, contact force due contact pressure and friction stresses). Figure 18 shows the contact patch between the pantograph strip and the contact wire as there is a sliding phenomenon between two components

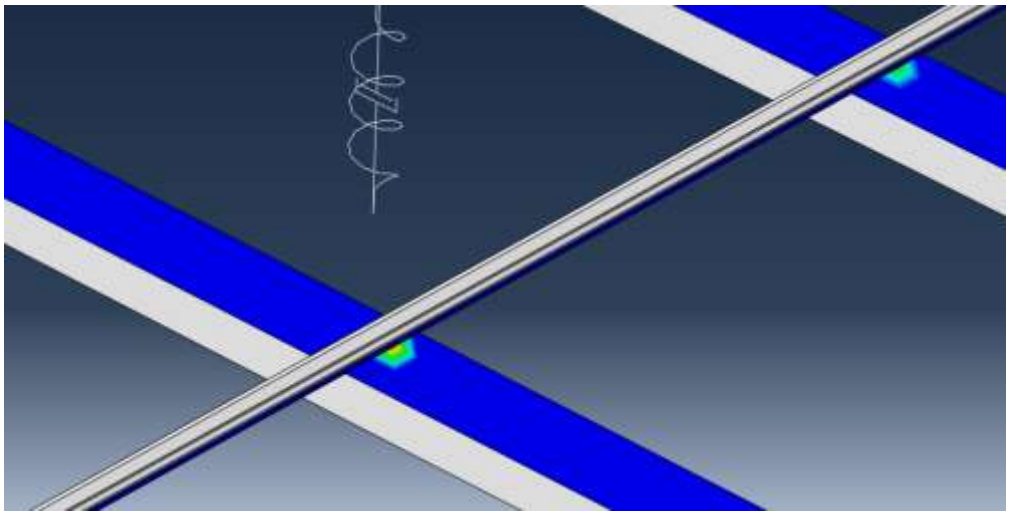

Figure 18. Contact patch between the pantograph contact strip and the contact wire as there is a sliding phenomenon between two components.

4.3 Pantograph -head vertical displacement

Figure 19 represents the deflection of the pantograph-head. In Figure 19. (a), the static response shows negligible values of the vertical deflection of the pantograph head as the dynamic uplift force is not yet activated. However, the activation of the dynamic uplift force results into the fluctuation of the vertical deflection of the pantograph head. As it is easy to observe in Figure 19. (b), (c); and (d), the pantograph head deflection increases progressively from 8.483 e -05 to 80 mm as the rail vehicle moves from a state of rest with a single velocity taken into account. To make it clear, for Figure 19.a) shows the pantograph head positioned in static position, b) shows pantograph displacement at a time equal 5.95 86e-2 seconds with the maximum displacement value of 12 mm, c) shows the pantographs displacement at time of 8.861e-2 seconds with the maximum deflection of 30.42 mm and C) shows the pantograph at time equal to 0.1134 seconds and the maximum displacement value of around 80 mm.

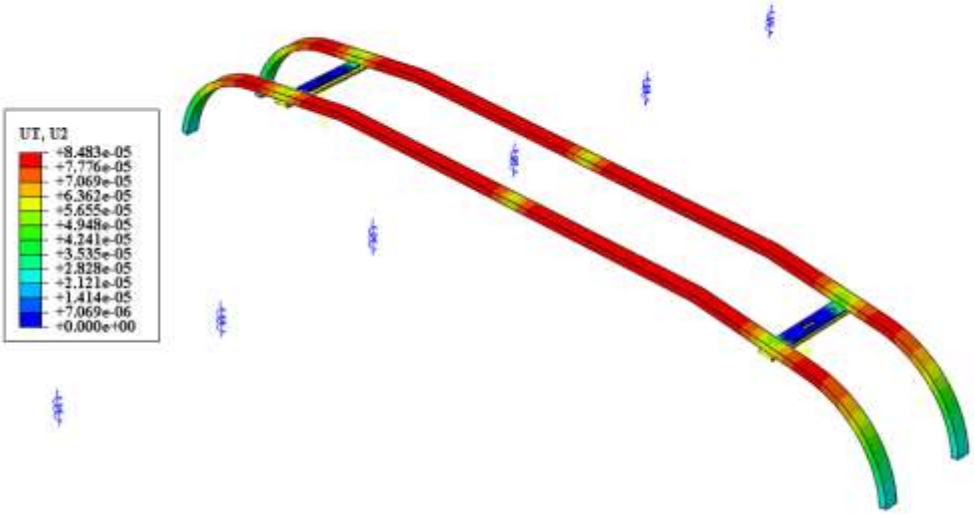
UT, U2
+8.483e-05
+7.776e-05
+7.069e-05
+6.362e-05
+5.655e-05
+4.948e-05
+4.241e-05
+3.535e-05
+2.828e-05
+2.121e-05
+1.414e-05
+7.069e-06
+0.000e+00

(a)

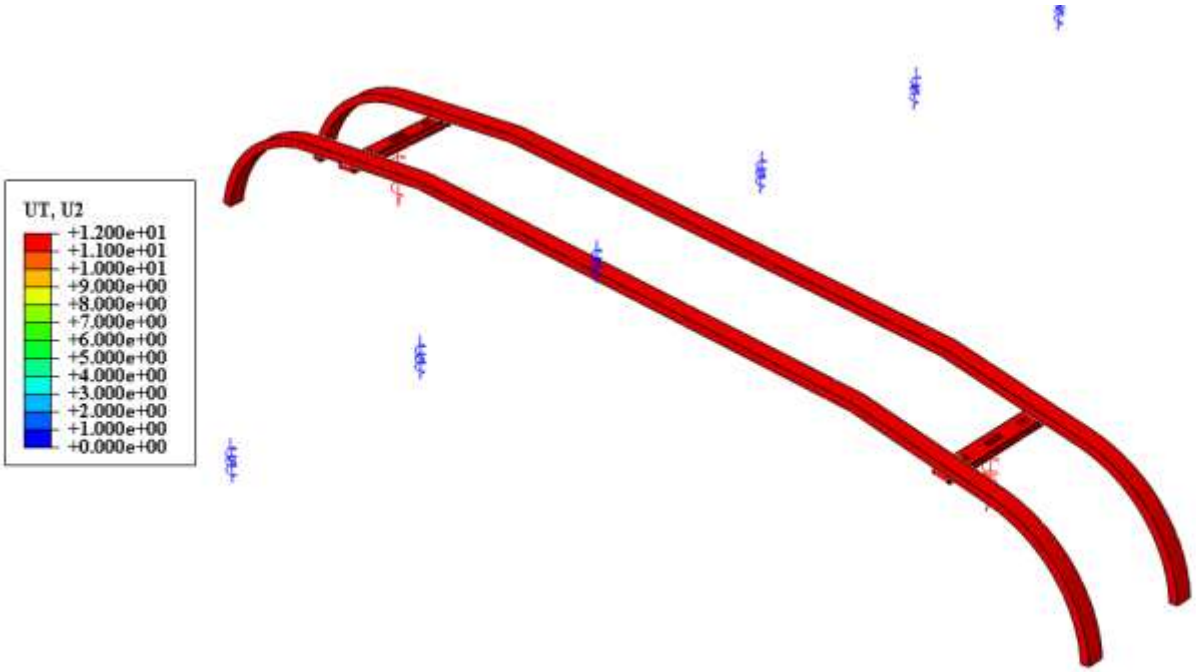
UT, U2
+1.200e+01
+1.100e+01
+1.000e+01
+9.000e+00
+8.000e+00
+7.000e+00
+6.000e+00
+5.000e+00
+4.000e+00
+3.000e+00
+2.000e+00
+1.000e+00
+0.000e+00

(b)

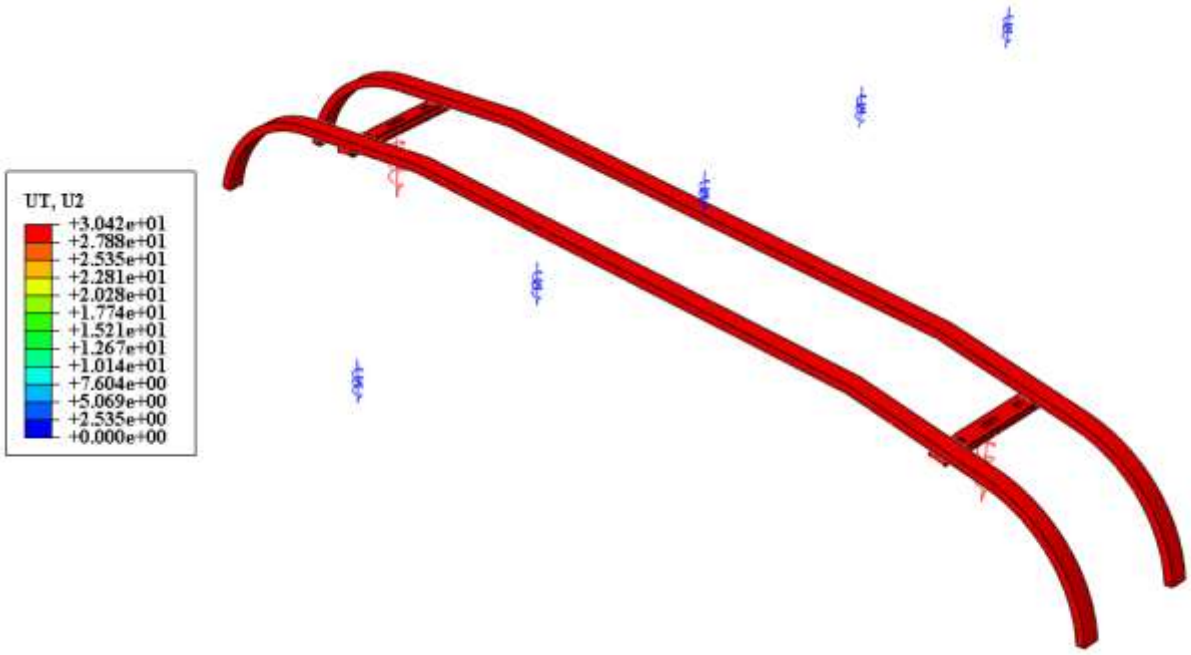

(c)

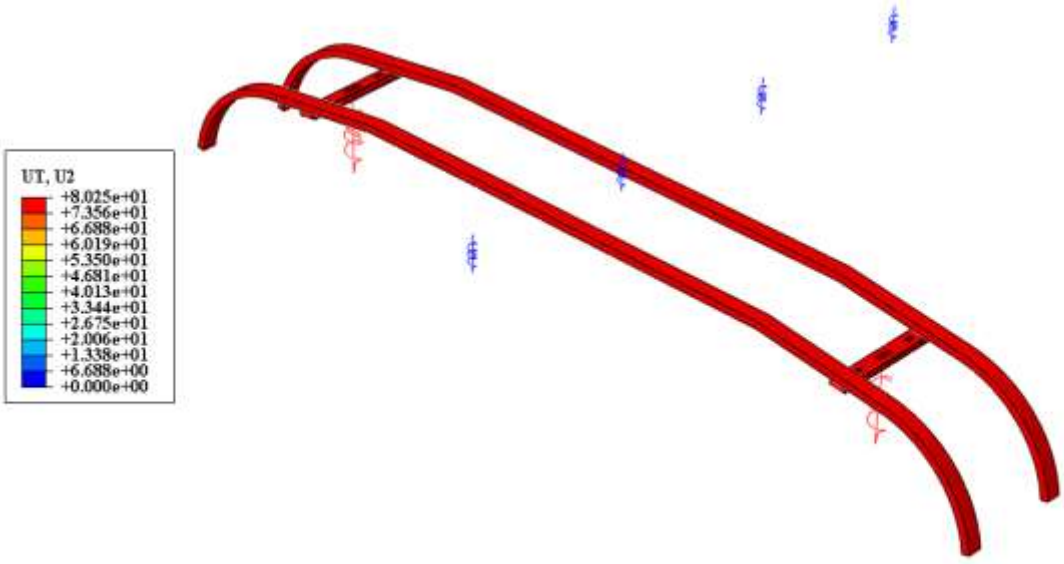

(d)

Figure 19. Response of Pantograph –head deflections fringes. (a) Deflections of the pantograph head at static state; (b); (c); (d) Variation of the pantograph head deflection when an uplift force is applied.

4.4 Friction-current -dependent Contact pressures simulation at various passengers' capacity (considering the heating effect)

Different loading conditions of the rail vehicle are considered referring to AA-LRTS systems rail vehicle passengers' capacity. It leads to running different finite elements models to capture the effects of rail vehicle overloading on the thermal behavior of the interacting components and hence present the effects of thermal behavior variation on wear of the system contacting components.

Relevant results from FEM models are extracted at each time increment by using the scripting techniques. Python scripting codes are developed to extract simulated results from FEM Output Data Base (ODB).i.e. (Contact pressures, slip velocity, slip distance, normal contact forces). In addition FEM history output reports are also generated to extract time history results (contact area, contact forces due to contact pressure and friction stresses,). Figure 20 below represents the simulations results of the contact pressures. (a) Depicts the viewport of the contact pressures; (b) Enlarged view of contact pressures at contact region; (c) represents the Curves of contact pressures variations against time at different passenger's capacity. Contact Pressures can be used to calculate the wear depth.

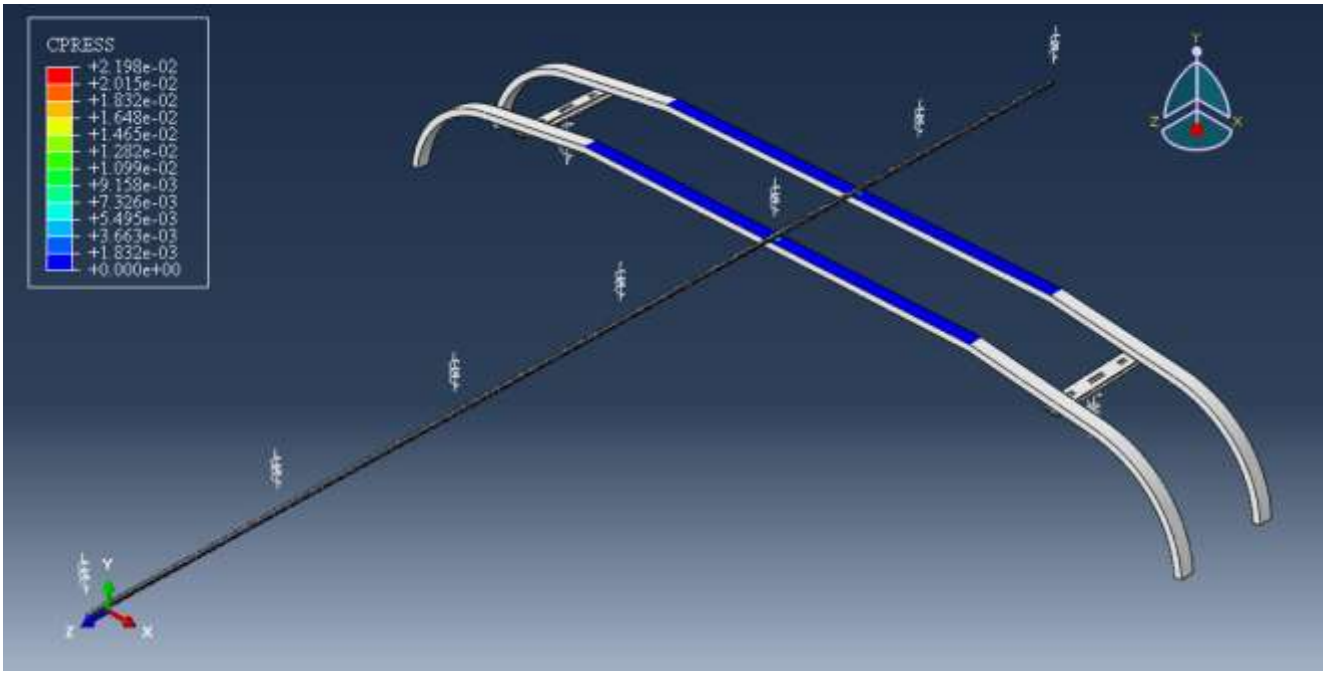

(a)

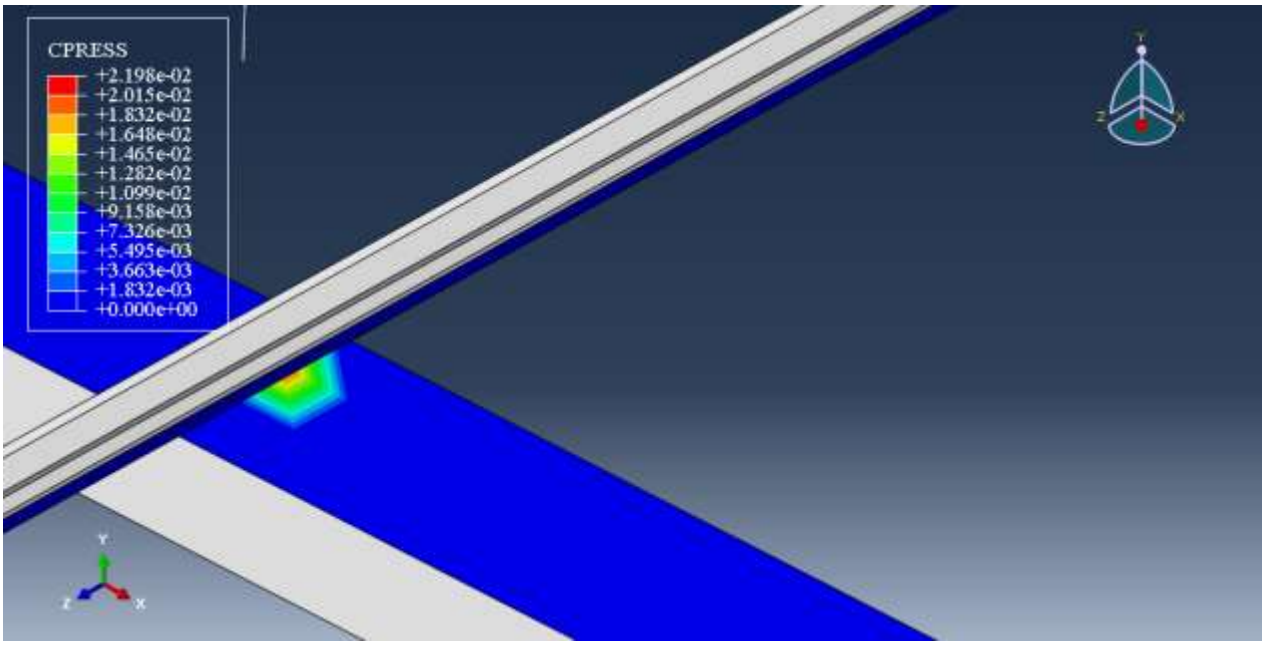

(b)

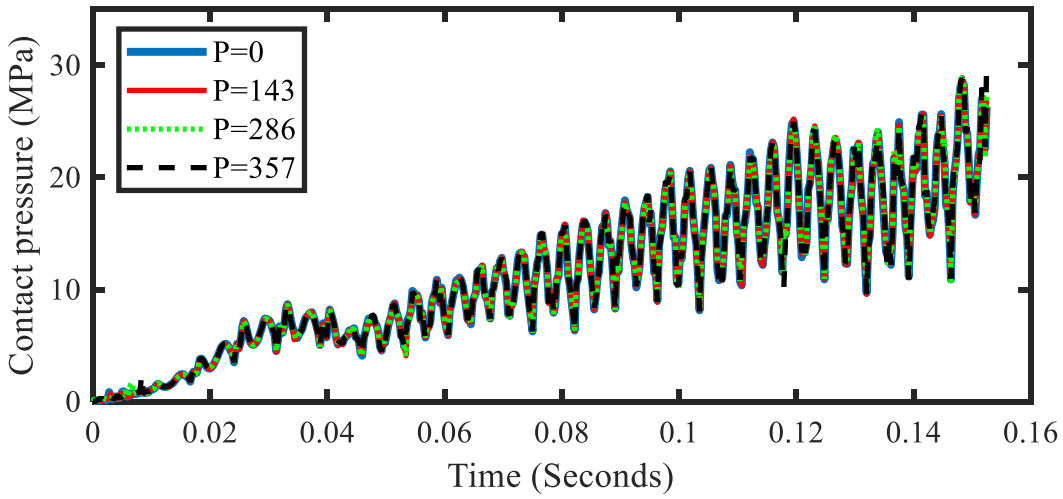

(c)

Figure 20. Contact pressures results, (a) viewport a full model showing the contact pressures; (b) Enlarged view of contact pressures at contact region; (c) Curves of contact pressures variations against time at different passenger's capacity. P represents the number of passengers and the value of P equals 0,143,286,357 was used as per reference of AA-LRTS operation parameters.

4.5 Temperatures variation on the pantograph and contact wire

The fluctuation of the current collected by the pantograph from the contact wire of the catenary while the rail vehicle is moving results in the temperature change of the interacting components. The passengers' capacity variation causes a significant change of the thermal behaviour of the railway power collection components due to great change of the power consumption which hence results in temperature rise. Figure 21shows the temperature variation of the pantograph strip and the contact wire at various rail vehicle passengers' capacity. It is obvious that the temperature of the components rises with increase in number of passengers.

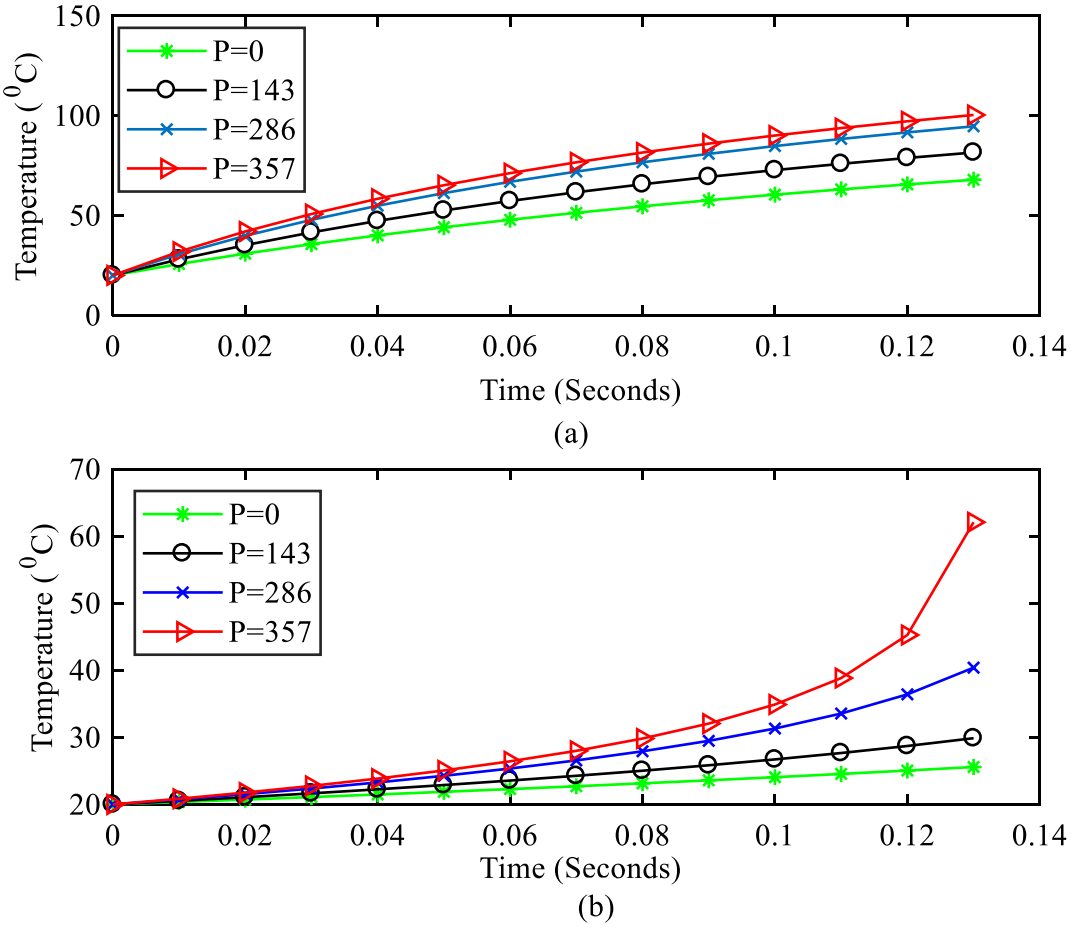

Figure 21.Temperature variation of the pantograph and contact wire. (a) Temperature of the pantograph strip; (b) Temperature of the contact wire. P represents the number of passengers.

4.6 Contact wire wear calculation

4.6.1 Contact normal forces on the contact wire

The wear volume model input parameters include normal contact forces of the pantograph-catenary, the hardness of the material under study and the wear coefficient of the mating materials under study. The sliding distance and the slip velocities are also the important input parameters to the wear model as the adopted model undergoes fully sliding phenomenon. The parameters like material hardness, wear coefficient are retrieved from literatures as was described in previous sections [55],[56] whereas the other parameters like contact pressures and contact normal forces are the outputs of the FE model of the pantograph-catenary simulated in ABAQUS software package. Figure 22 shows the contact force results. Various passenger's capacity are taken into consideration. As it is easy to observe, the contact wire experiences variation in contact forces at different passengers' capacity.

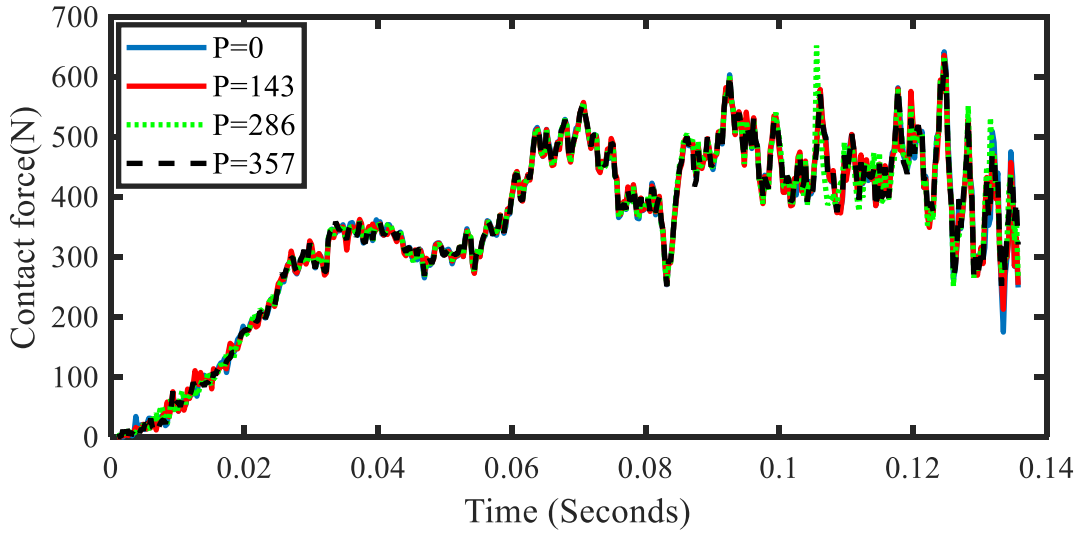

Figure 22. Pantograph-catenary normal contact forces at different rail vehicle passengers 'capacity. P represents the number of passengers.

4.6.2 Estimation of contact wire wear volume

Applying the Archard wear model, the contact conductor wear volume was estimated. The Archard wear Equation (19) was utilized for the contact conductor wear calculation. Figure 23 and Figure 23 demonstrate the wear volume of the contact conductor at different time increments. It is noteworthy to see that fluctuation in passengers' capacity results in variation of the wear volume

as time goes on whenever a train in moving from one point to another. The fluctuation in passengers' capacity results in dramatic change of the pantograph strip and contact conductor temperatures which in turn affect the thermal behavior of the sliding matting parts and be the source of contact conductor degradation due overheating.

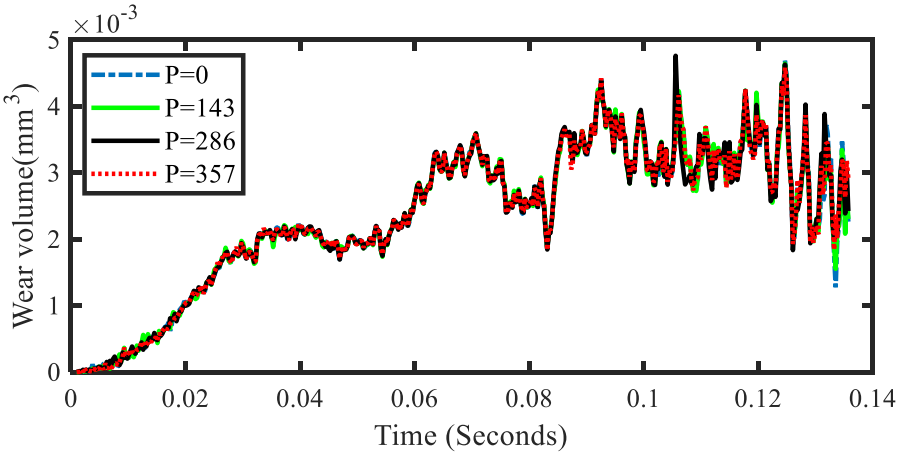

Figure 23. Contact conductor wear volume caused by pantograph strip 1 against time increment at different passengers' capacity. P represents the number of passengers.

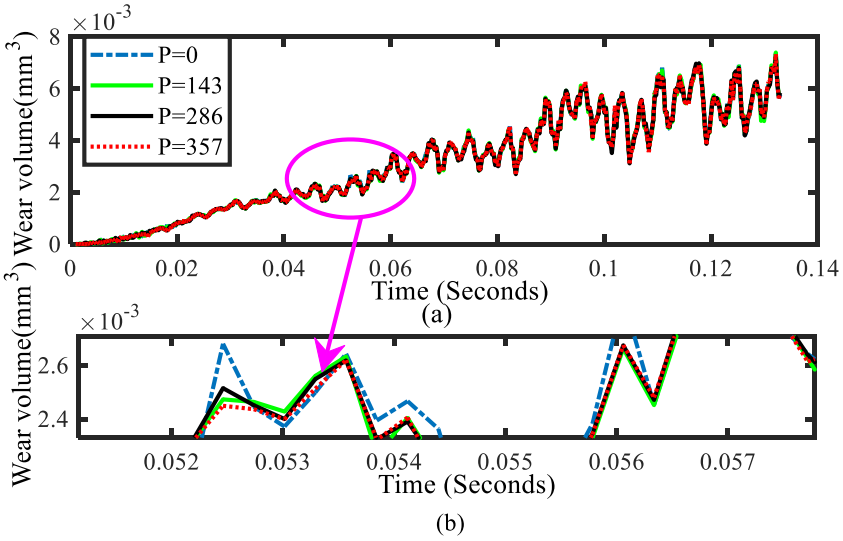

Figure 24. Contact conductor wear volume caused by pantograph strip 2 against time increment at different passenger capacities. (a) Contact conductor wear volume at pantograph contact strip 2. (b) Magnification of Figure (a) portion as demonstrated by the pink sphere and arrow, to show the significance of the passengers' capacity fluctuation on the wear of the contact conductor.

4.6.3 Estimation of contact conductor total wear volume

The total wear volume is the summation of individual wear volumes. It is the amount of wear experience by the contact conductor during the period of simulation meaning to say during the total running period of the train when it is moving from one point to another. Equation (20) was utilized to estimate the total wear volume of the contact conductor with respect to passenger mass. A passenger average mass of 60 kg was used in the current conducted research. As it is clearly obvious in Figure 25 (a) and (b), the wear of the contact conductor increases with the increase in passengers' mass.

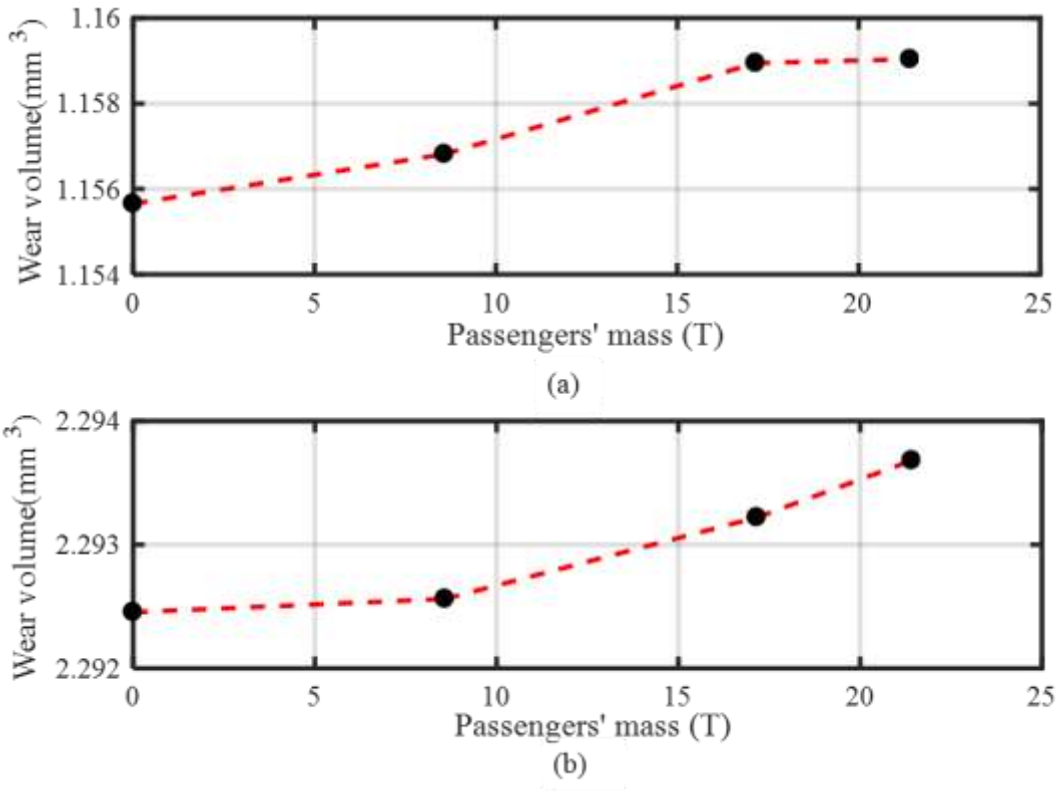

Figure 25. Total wear volume on the contact conductor against passengers' mass. (a) Total wear volume on the contact conductor caused by pantograph contact strip 1; (b) Total wear volume on the contact conductor caused by pantograph contact strip 2.

4.6.4 Estimation of contact wire wear depth

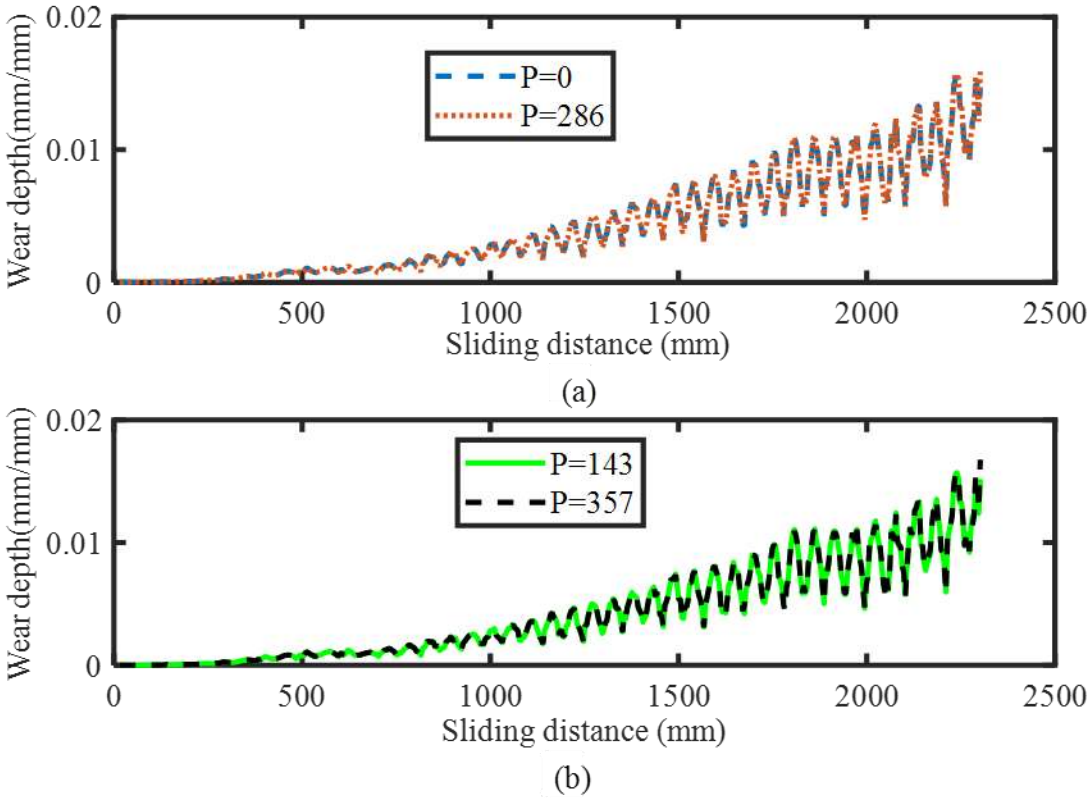

Figure 26. Wear depth along the contact wire against the sliding distance at various passengers 'capacity. (a) Wear depth when P= 0 and P= 286; (b) Wear depth wen P= 143 and P=357. P represents the number of passengers.

The wear depth of the contact conductor describes its reduction in diameter along its length. Figure 26 26 shows that the fluctuation in rail vehicle passengers' mass has the influence on the wear behavior of the contact wire and the wear depth of the contact wire increases with the increase in Passengers' capacity.

4.6.5 Results discussion and validation

The passenger capacity fluctuation has a great effects on the rail vehicle tractive effort as well as the rail vehicle power consumption. As it is depicted in Figure 15, the increase in rail vehicle passenger capacity from empty to overload capacity taking into account the average passenger's mass of 60 kg causes the increase of rail vehicle power consumption as well the increase of rail vehicle tractive effort. It is perfectly obvious in the Figure 15 that at the maximum number of 357

of rail vehicle passengers' capacity when the rail vehicle is overloaded the rail vehicle experiences the maximum values of power consumption as well the maximum values of tractive efforts.

Figure 16 also shows remarkable increase in the voltage drop at the catenary system as the number of passengers increase from 0 to 357 passengers and the rail vehicle is moving from one feeding substation to another.

Another import result is the vertical displacement of the pantograph head as the train is moving and the pantograph strip sliding along the contact wire of the catenary. As it shown by the Figure 19 (a); (b); (c) and (d), the vertical displacement of the pantograph head varies from 8.483 e-5 mm as time equal to zero seconds (meaning to say the rail vehicle is at rest) to a value of around 80 mm when the rail vehicle moves 0.1134 seconds and a vertical up-lift force of 100 N is applied on the pantograph. Moreover ,the results of the current research also showed that increasing the rail vehicle passengers' capacity from empty car to an overloaded car (i.e. from 0 to 357 passengers), increased the current to be drawn by the moving rail vehicle by 47%, Figure 9.(a);(b);(c);(d). It is crucial to note that the increase in the current drawn promoted the temperature rise of the pantograph-catenary interaction components once a dynamic simulation was performed using thermal robustness simulation techniques. As shown by the Figures 11, 12, 15 and 16, the increase in passengers' capacity resulted in the average increase of 0.24 %, 0.31 %, 0.29% and 0.20% of the contact pressures, contact forces, total wear volume and the total wear depth on the contact conductor respectively with the pantograph moving along the contact conductor and the rail vehicle moving between two adjacent feeding substations distancing of 2 Km.

The validation of the model used in this research is performed by comparing the contact forces obtained in this model and the ones obtained in [45] provided no control on the contact forces was applied on both models. Figure 22 shows the results of the contact forces in the current model whilst the results of contact forces for validation purpose are shown in Figure 11 of reference [45]. It was observed that the outcome of both models contact force results presented the contact forces absolute values ranging from 0 N to 700 N and this provided a better agreement between 2 models. Moreover, a comparison was made between the pantograph vertical deflection (pantograph head uplift in this case) obtained in this model and the ones obtained in the model analyzed in research [46]for the sake of relevant and additional validation of the current research. Here, the maximum pantograph head vertical displacement of around 90 mm is observed in in model of used in research

[46] while the pantograph head vertical displacement value of around 80 mm is observed in the current research model. A deviation of around 10 mm is remarked in both models. This is due to that in research [46], the equivalent uplift force generated by frictional force is considered and the latter is not taken into consideration for the current research. Moreover, It is worth to note that the additional uplift force enhances the interaction between the pantograph and the catenary under the friction condition and this results in further increase of the pantograph head displacement as it is shown in research [46]. Further validation is also made by comparing the contact point temperatures values on the pantograph and catenary obtained in this research and the temperatures values obtained in the research [60]. It is obvious that the temperatures values in both models represent similar tendency of temperatures rise from 20^0C to the value around 100^0C and this give another god credit to the results obtained in the currents research.

5 Conclusions, Recommendations and Future works

In this research, a study was undertaken to investigate the effect of train energy consumption on the damage of the catenary contact conductor. A finite element model approach was utilized to analyze the dynamic interaction between the pantograph and the catenary by taking into account the change in rail vehicle passengers' capacity as an important input parameter. Using the thermal robustness dynamic simulation technic, it was shown that the fluctuation in rail vehicle passengers' capacity has a significance influence on the rail vehicle energy consumption, which results into temperature rise of both the contact conductor and the pantograph strip. The temperature rise showed a great influence on thermal behavior change of the interaction components due to joule's effect and this led to the life degradation of the mating components.

Overall results showed that increased rail vehicle passengers' capacity from empty car to overloaded car increased the current drawn by the moving rail vehicle by 47% which in turn results into 20 to 100^{o}C of temperature increase. The former caused the average increase of 0.24%, 0.31%, 0.29% and 0.20% in contact pressures, contact forces, total wear volume and total wear depth on the contact conductor, respective It is worth to note that the current research has considered the constant speed of the rail vehicle in operation regardless the fluctuations in train passengers' capacity. However, the future work recommend the consideration of different train's speed and a combination of trains on the line so as to give a tangible overview and high accuracy of the expected results. Moreover, mesh independent test is suggested for the future research for optimizing the mesh size and verify the accuracy of the results.

References

[1] "Global Energy Outlook 2015," 2015.

[2] C. R. G. Limited, "Addis Ababa Light Rail Transit(AA-LRT) Project,North-South line," 2009.

[3] J. Wang and H. A. Rakha, "Electric train energy consumption modeling," *Appl. Energy*, vol. 193, pp. 346–355, 2017.

[4] C. Fiori, K. Ahn, and H. A. Rakha, "Power-based electric vehicle energy consumption model : Model development and validation," *Appl. Energy*, vol. 168, pp. 257–268, 2016.

[5] F. E. Gbologah, Y. Xu, M. O. Rodgers, and R. Guensler, "Demonstrating a Bottom-Up Framework for Evaluating Energy and Emissions Performance of Electric Rail Transit Options," no. September 2016, 2014.

[6] E. Commitee, "Development of Multibody Pantograph and Finite Element Catenary Models for Application to High-speed Railway Operations Pedro Cabaço Antunes Thesis to obtain the Master of Science Degree in Mechanical Engineering Examination Commitee," 2012.

[7] V. Ungureanu and A. Dósa, "methods for simulating the kinking of the rail-sleeper assembly using the SCfj program," *Railw. PRO*, 2011.

[8] A. D. Depa, *M* ul t ib o d y Dy n a m i c S i m ul a t i o n in P ro du c t Deve l o p me n t T o bi a s L ar ss o n. 2001.

[9] Z. Liu, *Measures to Enhance the Dynamic Performance of Railway Catenaries*. 2017.

[10] B. H. I. Andrews, M. Sc, and P. D. Member, "Third paper Calculating the Behaviour of an Overhead Catenary System for Railway Electrification," vol. 179, no. 25.

[11] and C. S. Yanyan Zhang 1, Yongzhen Zhang 1, 2, "Arc Discharges of a Pure Carbon Strip Affected by Dynamic Contact Force during," 2018.

[12] Y. Y. Zhang, Y. Z. Zhang, S. M. Du, C. F. Song, Z. H. Yang, and B. Shangguan, "Zhang YY, Zhang YZ, Du SM, Song CF, Yang ZH, Shangguan B, Tribological properties of pure carbon strip affected by dynamic contact force during current-carrying sliding, Tribology

International (2018), doi: 10.1016/j.triboint.2017.12.032.," 2018.

[13] L. I. N. Xiu-zhou, Z. H. U. Min-hao, M. O. Ji-liang, C. Guang-xiong, J. I. N. Xue-song, and Z. Zhong-rong, "Tribological and electric-arc behaviors of carbon / copper pair during sliding friction process with electric current applied," *Trans. Nonferrous Met. Soc. China*, vol. 21, no. 2, pp. 292–299, 2010.

[14] P. Taylor, "Vehicle System Dynamics : International Journal of Basic Analytical Study of Pantograph-catenary System Dynamics Basic Analytical Study of Pantograph-catenary System Dynamics," no. June 2013, pp. 37–41.

[15] Y. Yao, D. Zou, N. Zhou, G. Mei, and J. Wang, "A study on the mechanism of vehicle body vibration affecting the dynamic interaction in the pantograph – catenary system," vol. 3114, 2020.

[16] A. Facchinetti and S. Bruni, "Mechanics and Special issue on the pantograph – catenary interaction benchmark," no. April, pp. 51–54, 2015.

[17] P. Nåvik and A. Rønnquist, "Dynamic comparison of a railway catenary section upgrade by field measurement assessments," *Procedia Eng.*, vol. 199, pp. 2567–2572, 2017.

[18] F. H. Haugland, "Dynamic Behavior of a Full Scale Laboratory Model of a Catenary System by Measurements and Numerical Analysis," no. June, 2015.

[19] J. De Dios, J. D. D. Sanz, Á. Calvo, and D. Barbado, "Analysis of the capability of non-specific simulation software for studying the dynamic interaction between pantograph and rigid overhead conductor rail," *Transp. Res. Procedia*, vol. 33, pp. 187–194, 2018.

[20] M. Grandin and U. Wiklund, "M. Grandin and U. Wiklund, Wear phenomena and tribofilm formation of copper/copper-graphite sliding electrical contact materials, Wear, https://doi.org/10.1016/j.wear.2017.12.012," *Wear*, 2017.

[21] N. Zhou and W. Zhang, "Investigation on dynamic performance and parameter optimization design of pantograph and catenary system," vol. 47, pp. 288–295, 2011.

[22] T. Xin *et al.*, "Condition Based Railway Pantograph Dynamic Behavior Measurement and Fault Diagnosis," *IFAC-PapersOnLine*, vol. 51, no. 24, pp. 1083–1090.

[23] X. Xiong, C. Tu, and D. Chen, "Arc Erosion Wear Characteristics and Mechanisms of Pure Carbon Strip Against Copper Under Arcing Conditions," pp. 293–301, 2014.

[24] G. Bucca and A. Collina, "Tribology International Electromechanical interaction between carbon-based pantograph strip and copper contact wire : A heuristic wear model," *Tribiology Int.*, vol. 92, pp. 47–56, 2015.

[25] G. Pupke, F.nkt cables GmbH, Cologne, "Optimization and development of contact wire for high speed lines," vol. 7, no. 2, pp. 1–16.

[26] Aurubis, "Chemical Compostion of CuAg0.04(OF) / CuAg0.1(OF)," vol. 04, pp. 0–1.

[27] S. A. and D. Tilahun, "Sliding wear and Corrosion Resistance of Train Overhead Line Contact Wire," *J. EEA, Vol. 34, June 2016*, 2016.

[28] K. Shibata, T. Yamaguchi, Y. Yao, N. Yokoyama, J. Mishima, and K. Hokkirigawa, "Friction and Wear Properties of Copper/Carbon/RB Ceramics Composite under Electrical Current," *Tribol. Online*, vol. 4, no. 5, pp. 131–134, 2009.

[29] N. A. M. Tahir, M. F. Bin Abdollah, N. Tamaldin, H. Amiruddin, and M. R. Bin Mohamad Zin, "A brief review on the wear mechanisms and interfaces of carbon based materials," *Compos. Interfaces*, vol. 25, no. 5–7, pp. 491–513, 2018.

[30] T. Wajima, "Environmentally Friendly Solutions for Railway Systems," vol. 57, no. 5, pp. 179–183, 2008.

[31] S. Feng, "Research Status and Development Trend of Pantograph Contact Strip Materials," vol. 06040, pp. 0–4, 2016.

[32] M. Burkhardt, L. Rossi, and M. Boller, "Diffuse release of environmental hazards by railways," *Desalination*, vol. 226, no. 1–3, pp. 106–113, 2008.

[33] Y. Cha, *Airborne Particles in Railway Tunnels*. 2018.

[34] S. Midya, D. Bormann, A. Larsson, T. Schütte, and R. Thottappillil, "Understanding Pantograph Arcing in Electrified Railways – Influence of Various Parameters," 2008.

[35] T. Power and S. Key, "Pantograph and catenary system with double pantographs for high-

speed trains at 350 km/h or higher," vol. 19, no. 1, pp. 7–11, 2011.

[36] P. Taylor, W. M. Zhai, and C. B. Cai, "Vehicle System Dynamics : International Journal of Vehicle Mechanics and Mobility Effect of Locomotive Vibrations on Pantograph- Catenary System Dynamics," no. October 2014, pp. 37–41, 2007.

[37] G. Wu, W. Wei, G. Gao, J. Wu, and Y. Zhou, "Evolution of the electrical contact of dynamic pantograph – catenary system," *J. Mod. Transp.*, vol. 24, no. 2, pp. 132–138, 2016.

[38] P. H. Train, C. Park, Y. K. Yonghyeon, and C. J. Paik, "Development of Force Sensor to Measure Contact Force of," pp. 488–492.

[39] J. S. Kim, "An experimental study of the dynamic characteristics of the catenary-pantograph interface in high speed trains," *J. Mech. Sci. Technol.*, vol. 21, no. 12, pp. 2108–2116, 2007.

[40] A. S. Researcher and R. D. Division, "Estimation of W ear and Strain of Contact W ire Using Contact Force of Pantograph," vol. 48, no. 3, pp. 170–175, 2007.

[41] S. Hayes, D. I. Fletcher, A. E. Beagles, and K. Chan, "Effect of contact wire gradient on the dynamic performance of the catenary pantograph system," *Veh. Syst. Dyn.*, vol. 0, no. 0, pp. 1–23, 2020.

[42] W. Chu and Y. Song, "Study on Dynamic Interaction of Railway Pantograph – Catenary Including Reattachment Momentum Impact," pp. 18–33, 2020.

[43] G. Bucca and A. Collina, "A procedure for the wear prediction of collector strip and contact wire in pantograph – catenary system," vol. 266, pp. 46–59, 2009.

[44] H. J. Yang, G. X. Chen, G. Q. Gao, G. N. Wu, and W. H. Zhang, "Experimental research on the friction and wear properties of a contact strip of a pantograph – catenary system at the sliding speed of 350 km / h with electric current," pp. 4–10, 2014.

[45] C. M. Pappalardo, M. D. Patel, B. Tinsley, and A. A. Shabana, "Contact force control in multibody pantograph / catenary systems," vol. 230, no. 4, pp. 307–328, 2016.

[46] G. Chen, Y. Yang, and Y. Yang, "Prediction of dynamic characteristics of a pantograph-catenary system using the displacement compatibility," pp. 5405–5420, 2017.

[47] D. Seimbille, "Design of power supply system in DC electrified transit railways - Influence of the high voltage network," 2014.

[48] C. © 2018 S. J. U. P. P. by E. Inc., *Principles of Railway Location and Design,Traction Calculation*. 2018.

[49] K. Matsuoka and S. Member, "Energy Saving Technologies for Railway Traction Motors," pp. 278–284, 2010.

[50] M. Popescu and A. Bitoleanu, "A Review of the Energy Efficiency Improvement in DC Railway Systems," 2019.

[51] M. Kondo and D. Ph, "Development of T otally Enclosed Permanent Magnet Synchronous Motor Totally," vol. 49, no. 1, pp. 16–19, 2008.

[52] J. F. Archard and W. Hirst, "The Wear of Metals under Unlubricated Conditions," pp. 397–410, 1956.

[53] S. Contacts and M. Encounters, "Contact and Rubbing of Flat Surfaces," vol. 981, no. January 1953, 2004.

[54] J. J. Kauzlarich and J. A. Williams, "Archard wear and component geometry," vol. 215, pp. 387–403.

[55] S. Derosa, P. Nåvik, A. Collina, G. Bucca, and R. Anders, "A heuristic wear model for the contact strip and contact wire in pantograph – Catenary interaction for railway operations under 15 kV 16 . 67 Hz AC systems," vol. 457, 2020.

[56] W. E. Bring and Y. O. U. Forward, "Overhead contact wire,from cathode to catenary systems,Railway broncure."

[57] A. A. E.-W. & N.-S. (Phase I. L. R. T. P. Standard, Professional Technical, "Contract Line," no. Phase I.

[58] 目录Catalog. Co.Ltd, Changchun Railway Vehicles, "Operation and Maitenance Manual for 70% Low Floor Light Rail Vehicle Project of Addis Ababa, Ethiopia."

[59] M. Schaub and B. Simeon, "Mathematical and Computer Modelling of Dynamical

Systems : Methods , Tools and Applications in Engineering and Related Sciences Pantograph-Catenary Dynamics : An Analysis of Models and Simulation Techniques," no. December 2014, pp. 37–41, 2010.

[60] Z. Y. and G. G. Guangning Wu, JieWu, Wenfu Wei *Yue Zhou, "Characteristics of the Sliding Electric Contact of Pantograph/Contact wire System in Electrical Railways," 2018.

Appendices

Appendix A: Pantograph-contact wire temperatures fringes variations

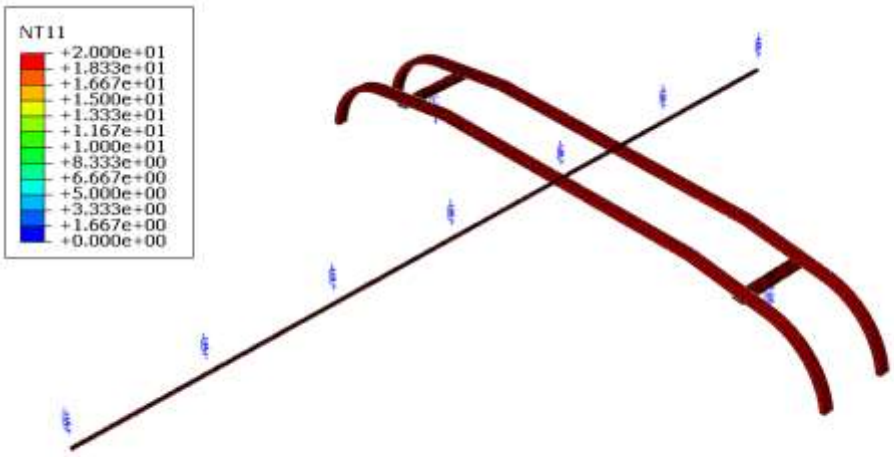

(a)

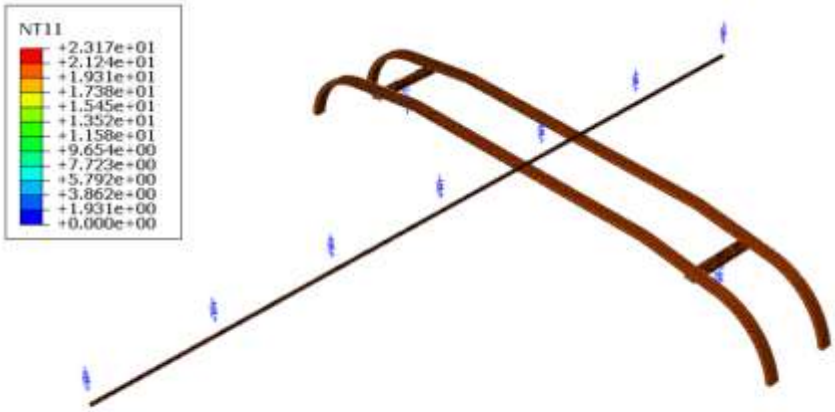

(b)

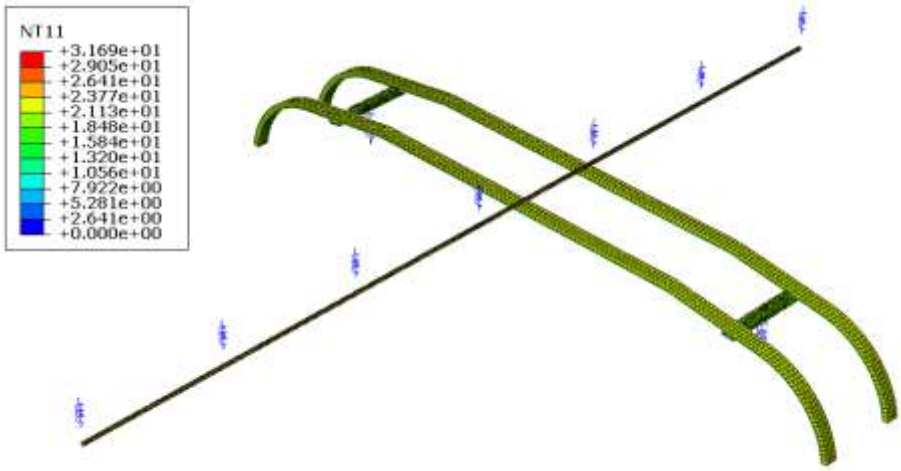
NT11
+3.169e+01
+2.905e+01
+2.641e+01
+2.377e+01
+2.113e+01
+1.848e+01
+1.584e+01
+1.320e+01
+1.056e+01
+7.922e+00
+5.281e+00
+2.641e+00
+0.000e+00

(c)

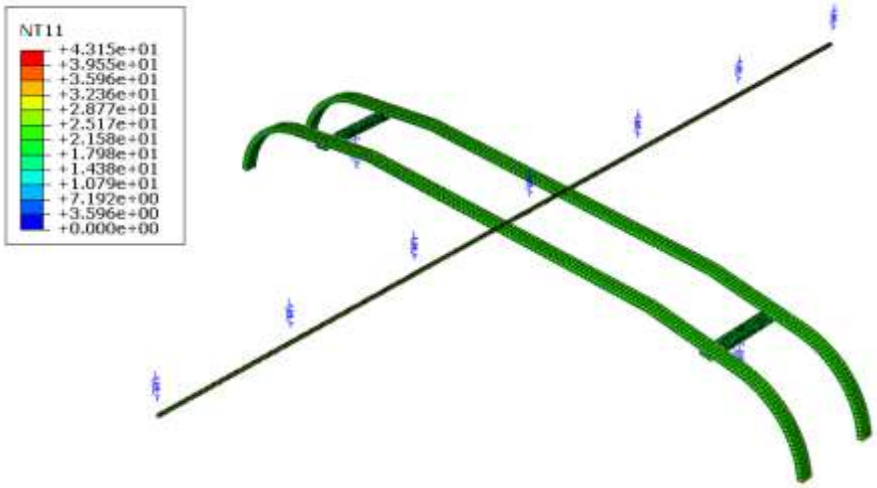
NT11
+4.315e+01
+3.955e+01
+3.596e+01
+3.236e+01
+2.877e+01
+2.517e+01
+2.158e+01
+1.798e+01
+1.438e+01
+1.079e+01
+7.192e+00
+3.596e+00
+0.000e+00

(d)

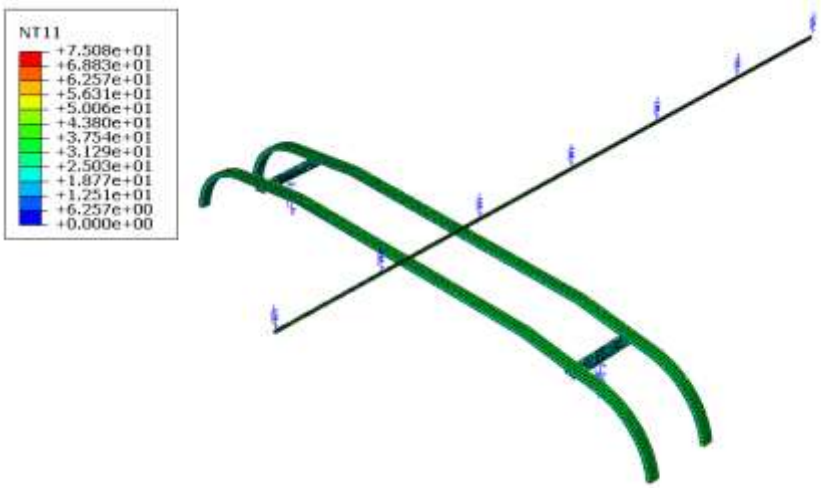

(f)

Pantograph-catenary temperature fringes. Figure (a); (b); (c); (d) and (f)

Appendix B: Power flow analysis Matlab scripting codes

1. Pantograph temperature variation Matlab scripting codes

```
clc;
close all;
 r=[];
B=[];
C=[];
E1=[];
E2=[];
E3=[];
E4=[];
D=[];


dtt=0.1:0.1:5
DT=dtt'
iteration=1:50;
Tm=20;
To =20;
```

```
%r= 3000e-8;
% Pantograph strip surface area
A = 0.1043848;
% Concevtdive heat coedfficient
h = 100;
% Emissivity
E = 0.81;
% stefan bolzman coefficient
Q = 5.67e-8;
% Pantograph mass
M = 3.5490832;
% Specific heat coefficient
Cp = 710;
d=-5e-4;
%Rn = r*(2.60962)/A;
Vt11=1497.3;

for i=1:50

 for dt = 0.1:0.1:5
    It11=1000;
Tn = Tm + (((Vt11*It11*dt) - (h*A*(Tm - To))*dt - E*A*Q*(power(Tm,4)-(power(To,4)*dt)))/(M*Cp));
%Rn=Rn*(1+d*(Tn-Tm));
%Tn = Tm + ((((power(I,2))*Rn*dt) - (h*A*(Tm - To))*dt - E*A*Q*(power(Tm,4)-(power(To,4)*dt)))/(M*Cp));
%Rn=Rn*(1+d*(Tn-Tm));
EnergyStored= (M*Cp)*(Tn-Tm);
EnergyIN=(Vt11*It11*dt)/M*Cp;
EnergyOutCv=(h*A*(Tm - To))*dt;
EnergyOutRd= E*A*Q*(power(Tm,4)-(power(To,4)))*dt;
```

```
Tm;
Tn;
H=EnergyOutCv/A*(Tm-To)*dt;
 end
%Ar(i)=Rn;
B(i)=Tm;
C(i)=Tn;
Tm=Tn;
E1(i)=EnergyStored;
E2(i)=EnergyIN;
E3(i)=EnergyOutCv;
E4(i)=EnergyOutRd;


end
T=table(iteration',B',C',E1',E2',E3',E4',DT);
T.Properties.VariableNames                                                    =
{'iteration','PrevTemp','Wire_Temp','Energy_Stored','EnergyIN','Energy_outCV','Energy_outRD'
,'Time_Change','Conv_coef'}
fileName = 'Data.xlsx';
writetable(T,fileName)
winopen(fileName)
```

2. Contact conductor wire temperature variation Matlab scripting codes

```
clc;
close all;
Ar=[];
B=[];
C=[];
E1=[];
E2=[];
E3=[];
```

```
E4=[];
D=[];
dtt=0.01:0.01:0.5;
DT=dtt';
iteration=1:50;
Tm=20;
To = 20;% Ambient temperature
r= 1.8e-8; %Resistivity of sliver copper-contact wire material (ohm-m)
% A = 0.1448325;
A=0.0176625;  % cross section area of the contact wire(m^2)
h = 25;
E = 0.023; % Emissivity coefficient of copper
Q = 5.67e-8; %Stefan Boltzmann coefficient of copper
M = 0.741; %Mass of Contact wire
Cp = 245; % Specific heat capacity(J/Kg.k)
d=0.00383;  % Thermal expansion coefficient
%Rn=0.000061;
Rn = r*(3)/A; %Resistance of contact wire(ohm)
for i=1:50
 for dt =0.1:0.1:5
  I=3154.1;
Tn = Tm + (((I^2*Rn*dt) - (h*A*(Tm - To))*dt - (E*A*Q*(Tm^4-To^4)*dt))/(M*Cp));
Rn=Rn*(1+d*(Tn-Tm));
EnergyStored= (M*Cp)*(Tn-Tm);
EnergyIN=((I^2)*Rn*dt);
EnergyOutCv=(h*A*(Tm - To))*dt;
EnergyOutRd= (E*A*Q*(Tm^4-To^4))*dt;
Tm;
Tn;
H=EnergyOutCv/A*(Tm-To)*dt;
 end
```

```
Ar(i)=Rn;
B(i)=Tm;
C(i)=Tn;
Tm=Tn;
E1(i)=EnergyStored;
E2(i)=EnergyIN;
E3(i)=EnergyOutCv;
E4(i)=EnergyOutRd;
end
T=table(iteration',Ar',B',C',E1',E2',E3',E4',DT);
T.Properties.VariableNames =
{'iteration','RESISTANCE','PrevTemp','Wire_Temp','Energy_Stored','EnergyIN','Energy_outCV'
,'Energy_outRD','Time_Change'};
fileName = 'Data.xlsx';
writetable(T,fileName)
winopen(fileName)
```

3. Train tractive efforts, train power, current voltage Matlab scripting codes

```
clc
clf
%script to estimate the total tractive effort of the train
%Addis Ababa Light Rail Transit (AA-LRT)
m=43000;      %Dead mass of the train
N1=0;        %Number of passengers zero sitting capacity
N2=143;     %Vehicle with half capacity of passengers
N3=286;      % vehicle with full seating capacity of passengers
N4=357;     %vehicle with overload capacity of passengers
%N5=500;
b=60;         %Average weight of a passenger
n=6;          %Number of axles
K=0.07;       %Drag efficient (dimensionless)
%V=800/36;     %Speed of the train (m/s)
```

```
V=0:0.1:25;      % speed change (m/s)
a=1;          %Linear acceleration of the train (m/s^2)
G=0.05;       %Percentage grade
e1=0.97;      %Traction motor Efficiency
e2=0.9;       %Transmission efficiency
E=e1*e2;      % Total efficiency of the traction

d1=N1*b;       %Total weight of the passengers (kg)
d2=N2*b;
d3=N3*b;
d4=N4*b;
%d5=N5*b;
M1=m+d1;       %Total mass of the train(kg)
M2=m+d2;
M3=m+d3;
M4=m+d4;
%M5=m+d5;

W1=M1;
W2=M2;
W3=M3;
W4=M4;
%W5=M5;

w1=W1/n;       % weight per axle
w2=W2/n;
w3=W3/n;
w4=W4/n;
%w5=W5/n;

y=0.33; %Adhesion coefficient
```

```
g=9.81; %Acceleration due to gravity
% R1=M1*(0.6+ (20/W1) +0.01.*V+(K/w1*n).*V.^2)*0.005;  %Using modified Davis Equation, o.005 is conversion from lb/t to N/kg
% R2=M2*(0.6+ (20/W2)+0.01.*V+(K/w2*n).*V.^2)*0.005;
% R3=M3*(0.6+(20/W3)+0.01.*V+(K/w3*n).*V.^2)*0.005;
% R4=M4*(0.6+(20/W4)+0.01.*V+(K/w4*n).*V.^2)*0.005;
% R5=M5*(0.6+(20/W5)+0.01.*V+(K/w5*n).*V.^2)*0.005;

%T=(1.1*M*a)+(0.098*M*G)+R;  %Tractive effort(N)
% T1s=M1*y*g;
% T2s=M2*y*g;
% T3s=M3*y*g;
% T4s=M4*y*g;
% T5s=M5*y*g;

% T1s=((1.1*M1*a)+(0.098*M1*G));
% T2s=((1.1*M2*a)+(0.098*M2*G));
% T3s=((1.1*M3*a)+(0.098*M3*G));
% T4s=((1.1*M4*a)+(0.098*M4*G)+R4);
% T5s=((1.1*M5*a)+(0.098*M5*G)+R5);

Pm=3000000;      %maximum power for EMU train
P1=zeros(1,length(V));
P2=zeros(1,length(V));
P3=zeros(1,length(V));
P4=zeros(1,length(V));
%P5=zeros(1,length(V));
for i=1:length(V)
   y1(i)=y/(1+0.01*V(i));
   T1s=M1*y1(i)*g;
   P1(i)=T1s*V(i)
```

```
  if P1(i)>=Pm
     P1(i)=Pm;
     T1(i)=(P1(i)/V(i))*E;
  else

     P1(i)=T1s*V(i)/E;
     T1(i)=T1s;
  end
  T2s=M2*y1(i)*g;
  P2(i)=T2s*V(i);
if P2(i)>=Pm

     P2(i)=Pm;
      T2(i)=(P2(i)/V(i))*E;
  else
     P2(i)=T2s*V(i)/E;
     T2(i)=T2s;
end

T3s=M3*y1(i)*g;
P3(i)=T3s*V(i);
if P3(i)>=Pm
   P3(i)=T3s*V(i);
     P3(i)=Pm;
     T3(i)=(P3(i)/V(i))*E;
else
     P3(i)=T3s*V(i)/E;
     T3(i)=T3s ;
end
T4s=M4*y1(i)*g;
P4(i)=T4s*V(i);
```

```
 if P4(i)>=Pm
      P4(i)=Pm;
     T4(i)=(P4(i)/V(i))*E;
   else
      P4(i)=T4s*V(i)/E;
      T4(i)=T4s  ;
 end
%   T5s=M5*y1(i)*g;
%   P5(i)=T5s*V(i);
%   if P5(i)>=Pm;
%        P5(i)=Pm;
%         T5(i)=(P5(i)/V(i))*E;
%    else
%        P5(i)=T5s*V(i)/E;
%        T5(i)=T5s;
%   end
end
%P=T.*(V./E);  % Power output
subplot(2,1,1)
plot(V,P1,'O--');
xlabel('speed (m/s)');
ylabel('Tractive effort (N)');
%title('Tractive effort for AA-LRT Trains with change in speed')
grid off;
 hold on;
 plot(V,P2);
 hold on;
 plot(V,P3);
 hold on;
 plot(V,P4);
 %hold on;
```

```
 legend('P=0' , 'P=134','P=286','P=357')
subplot(2,1,2)
 plot(V,T1,'O--');
xlabel('speed (m/s)');
ylabel('Tractive effort (N)');
%title('Tractive effort for AA-LRT Trains with change in speed')
grid off;
 hold on;
 plot(V,T2);
 hold on;
 plot(V,T3);
 hold on;
 plot(V,T4);
 %hold on;
 legend('P=0' , 'P=134','P=286','P=357')
```

4. Matlab script for total wear volume

```
%% Import data from spreadsheet
% Script for importing data from the following spreadsheet:
%    Workbook: E:\ADDIS ABABA\Rolling stock railway masters first sem\2018-2019 NOTES\Thesis\Commented thesis\Thesis typing\Correct figures\600\FS1\FS11.xlsx
%    Worksheet: Sheet1
% To extend the code for use with different selected data or a different
% spreadsheet, generate a function instead of a script.
% Auto-generated by MATLAB on 2020/12/17 01:15:58

%% Import the data
[~, ~, raw] = xlsread('E:\ADDIS ABABA\Rolling stock railway masters first sem\2018-2019 NOTES\Thesis\Commented thesis\Thesis typing\Correct figures\600\FS1\FS11.xlsx','Sheet1','A2:D5');
%% Create output variable
data = reshape([raw{:}],size(raw));
```

```
%% Create table
FS11 = table;
%% Allocate imported array to column variable names
FS11.P = data(:,1);
FS11.M = data(:,2);
FS11.T = data(:,3);
FS11.T2 = data(:,4);
%% Clear temporary variables
clearvars data raw;
subplot(2,1,1)
plot(FS11.P,FS11.T)
xlabel('Passengers mass (T)')
ylabel('Wear volume(mm^3)')
title('Total wear volume  due to pantograph-strip 1')
subplot(2,1,2)
plot(FS11.P,FS11.T2)
xlabel('Passengers mass (T)')
ylabel('Wear volume(mm^3)')
title('Total wear volume due to pantograph-strip 2')
% legend('Wear due to S1','Wear due to S2')
```

Appendix C: Python scripting codes to extract contact pressures, sliding distance, slip velocity.

1. Contact pressures extraction python scripting codes

```
myOdb = odbAccess.openOdb(path='C:\Users\Niringimana\Documents\scripting_ex\job-26-286.odb', readOnly=False)

#Get the two steps separately and call them step1 and step2

step1 = myOdb.steps['Step-3']

step2=myOdb.steps['Step-4']
```

```
#max_cpress=[]
#max_cshear1=[]
#max_cshear2=[]
fmcp=open('C:\Users\Niringimana\Documents\scripting_ex\max_cpress2.xls','w')
#Write headings for each columns: 'Step time','CPRESS','CSHEAR1','CSHEAR2' on same line.
[fmcp.write(str(titledata)+'\t') for titledata in ['Step time','CPRESS','CSHEAR1','CSHEAR2']]
fmcp.write('\n')
t0=0.0
for frame in step2.frames:

    steptime=t0+frame.frameValue

cpress,cshear1,cshear2=frame.fieldOutputs['CPRESS'],frame.fieldOutputs['CSHEAR1'],frame.fieldOutputs['CSHEAR2']
    timestep=frame.frameValue
    n_data=len(cpress.values)
    #Initialize the list all_cpress which will accept contact pressure data
    all_cpress=[]
    all_cshear1=[]
    all_cshear2=[]
    ## Let loop over each contact pressure data and extract it. Note: contact pressure data is extracted by using an attribute,data
    for  i in range(n_data):
```

```
cpress_value,c_sh1_value,c_sh2_value=cpress.values[i].data,cshear1.values[i].data,cshear2.valu
es[i].data

    #Append each contact pressure at the list, except if the value is zero (This allows us to
reduce the computation time)

    if cpress_value>0.00:

        all_cpress.append(cpress_value)

    if c_sh1_value>0.00:

        all_cshear1.append(c_sh1_value)

    if c_sh2_value>0.00:

  if all_cpress==[]:

    all_cpress=[0.0]

  if all_cshear1==[]:

    all_cshear1=[0.0]

  if all_cshear2==[]:

    all_cshear2=[0.0]

  max_cp=max(all_cpress)

  max_csh1=max(all_cshear1)

  max_csh2=max(all_cshear2)

  #max_cpress.append(max_cp)

  #max_cshear1.append(max_csh1)

  #max_cshear2.append(max_csh2)

  [fmcp.write(str(datavalue)+'\t') for datavalue in [steptime,max_cp,max_csh1,max_csh2]]
```

```
    fmcp.write('\n')
run_time=time.time()-start_time
fmcp.write(str(run_time))
# close the text file fmcp
fmcp.close()
```

2. Sliding distance extraction python scripting codes

```
myOdb = odbAccess.openOdb(path='C:\Users\Niringimana\Documents\scripting_ex\job-26-286.odb', readOnly=False)
#Get the two steps separately and call them step1 and step2
step1 = myOdb.steps['Step-3']
step2 = myOdb.steps['Step-4']
max_fslipeq = []
 [fmcp.write(str(titledata)+'\t') for titledata in ['Step time','FSLIPEQ ASSEMBLY_S_SURF/ASSEMBLY_M_SURF-1']]
t0=0.0
for frame in step2.frames:

        steptime=t0+frame.frameValue
        fslipeq = frame.fieldOutputs['FSLIPEQ  ASSEMBLY_S_SURF/ASSEMBLY_M_SURF-1']
        timestep=frame.frameValue
        n_data=len(fslipeq.values)
```

```
        all_fslipeq=[]
        for  i in range(n_data):
            fslipeq_value = fslipeq.values[i].data
            if fslipeq_value>0.00:
                all_fslipeq.append(fslipeq_value)
        if all_fslipeq==[]:
            all_fslipeq=[0.0]
        max_cp=max(all_fslipeq)
        #max_cpress.append(max_cp)
        #max_cshear1.append(max_csh1)
        #max_cshear2.append(max_csh2)
        #store this data in the file fmcp
        [fmcp.write(str(datavalue)+'\t') for datavalue in [steptime,max_cp]]
        fmcp.write('\n')
run_time=time.time()-start_time
fmcp.write(str(run_time))
# close the text file fmcp
fmcp.close()
# C:\Users\user\Documents\scripting_ex\PostProcessing_cpress.py
```